Department of Neuroscience and Biomedical Engineering

Convolution and model-based dose calculation methods in radionuclide and external-beam photon therapy

Joakim Pyyry

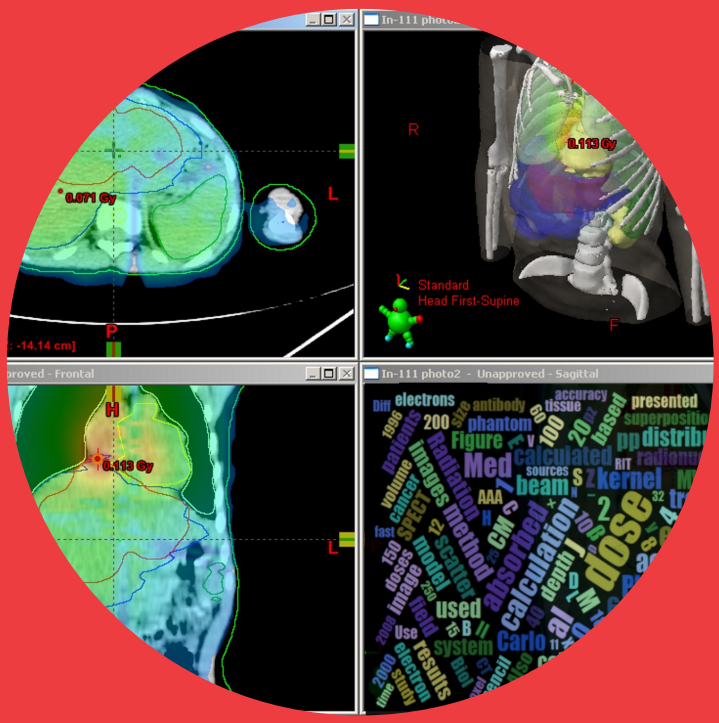

Aalto University

DOCTORAL DISSERTATIONS

Aalto University publication series
DOCTORAL DISSERTATIONS 57/2016

Convolution and model-based dose calculation methods in radionuclide and external-beam photon therapy

Joakim Pyyry

A doctoral dissertation completed for the degree of Doctor of Science (Technology) to be defended, with the permission of the Aalto University School of Science, at a public examination held at the lecture hall A1 of the school on 15 April 2016 at 12.

Aalto University
School of Science
Department of Neuroscience and Biomedical Engineering

Supervising professor
Professor Lauri Parkkonen, Department of Neuroscience and Biomedical Engineering, Aalto University, Finland

Thesis advisors
Visiting Professor Kalevi Kairemo, Department of Nuclear Medicine, The University of Texas MD Anderson Cancer Center, USA

Chief Physicist Mikko Tenhunen, HUCH Comprehensive Cancer Center, Finland

Preliminary examiners
Professor Dietmar Georg, Medical Radiation Physics and Oncotechnology, Medical University of Vienna, Austria

Dr. Mark Lubberink, PET centre, Uppsala University Hospital, Sweden

Opponent
Dr. Mark Konijnenberg, Nuclear Medicine, Erasmus Medical Center, Netherlands

Aalto University publication series
DOCTORAL DISSERTATIONS 57/2016

ISBN 978-952-60-6727-8 (printed)
ISBN 978-952-60-6728-5 (pdf)
ISSN-L 1799-4934
ISSN 1799-4934 (printed)
ISSN 1799-4942 (pdf)
http://urn.fi/URN:ISBN:978-952-60-6728-5

Unigrafia Oy
Helsinki 2016

Finland

NORDIC ECOLABEL
441 697
Printed matter

Aalto University

Abstract

Aalto University, P.O. Box 11000, FI-00076 Aalto www.aalto.fi

Author
Joakim Pyyry

Name of the doctoral dissertation
Convolution and model-based dose calculation methods in radionuclide and external-beam photon therapy

Publisher School of Science

Unit Department of Neuroscience and Biomedical Engineering

Series Aalto University publication series DOCTORAL DISSERTATIONS 57/2016

Field of research Medical Physics

Manuscript submitted 4 June 2015 **Date of the defence** 15 April 2016

Permission to publish granted (date) 19 August 2015 **Language** English

☐ **Monograph** ☒ **Article dissertation** ☐ **Essay dissertation**

Abstract

Radiotherapy is an established treatment modality of cancer. Radiation is delivered to the patients from internal or external sources. This thesis explores and introduces improvements to computational methods that are used in the application of internal and external radiotherapy. The aims of the work were to develop a general methodology for 3D treatment planning of internal radionuclide therapy, to apply 3D treatment planning to analyze radionuclide therapy cases, and to develop a pencil-beam dose kernel based calculation method for external photon therapy that also accounts for local variations in tissue material densities in 3D space.

The variability of biological uptake and clearance of the therapy agent were analyzed in various patients undergoing radionuclide therapy by serial single-photon emission computed tomography (SPECT), and estimates of absorbed doses were calculated. Patient-specific dose calculation with the dose kernel method was compared with the widely used MIRD S-factor model. Large inter-patient variation of biological clearance and localized differences for individual patients were observed. The dose estimates from the S-factor model and point dose kernel approach agreed on average, but at an individual patient level there were large variations between the methods.

For external photon therapy, an advanced pencil beam dose calculation method was developed. The resulting Analytical Anisotropic Algorithm (AAA) includes a density-scaling method of both lateral and depth-dependent components of the model. The results indicate generally good agreement between the calculations utilizing the presented method and Monte Carlo simulations in various heterogeneous geometries. Most of the observed discrepancies were within 2% (or 2~mm). The method is computationally very efficient and suitable for routine use in clinical setting.

Keywords radiotherapy, radionuclide, pencil beam, point kernel, treatment planning

ISBN (printed) 978-952-60-6727-8 **ISBN (pdf)** 978-952-60-6728-5

ISSN-L 1799-4934 **ISSN (printed)** 1799-4934 **ISSN (pdf)** 1799-4942

Location of publisher Helsinki **Location of printing** Helsinki **Year** 2016

Pages 149 **urn** http://urn.fi/URN:ISBN:978-952-60-6728-5

Tekijä
Joakim Pyyry

Väitöskirjan nimi
Konvoluutio- sekä mallipohjaiset annoslaskentamenetelmät isotooppi- ja ulkoisessa sädehoidossa

Julkaisija Perustieteiden korkeakoulu

Yksikkö Neurotieteen ja lääketieteellisen tekniikan laitos

Sarja Aalto University publication series DOCTORAL DISSERTATIONS 57/2016

Tutkimusala Sädehoitofysiikka

Käsikirjoituksen pvm 04.06.2015 **Väitöspäivä** 15.04.2016

Julkaisuluvan myöntämispäivä 19.08.2015 **Kieli** Englanti

☐ **Monografia** ☒ **Artikkeliväitöskirja** ☐ **Esseeväitöskirja**

Tiivistelmä

Sädehoito on laajasti käytössä oleva syövän hoitomuoto. Potilaita hoidetaan joko ulkoisilla tai sisäisillä säteilylähteillä. Väitöskirja käsittelee sekä sisäisen että ulkoisen sädehoidon laskennallisia menetelmiä. Tutkimuksessa kehitettiin yleinen menetelmä isotooppihoitojen kolmiulotteiseen annossuunnitteluun ja sovellettiin tätä menetelmää isotooppihoitojen annosten analysointiin. Lisäksi kehitettiin ulkoisen sädehoidon annoslaskentamenetelmä, joka huomioi epähomogeenisen väliaineen vaikutukset säteilyn kulkeutumisessa.

Tutkimuksessa analysoitiin isotooppihoitojen aktiivisuusjakaumia, isotooppien biologisia poistumia ja säteilyannoksia useissa potilastapauksissa SPECT-kuvantamisen avulla. Potilaskohtaisia annoslaskentoja suoritettiin konvoluutiomenetelmällä ja näitä verrattiin yleisesti käytössä olevan MIRD S -mallin tuloksiin. Analyysissä havaittiin isoja eroja potilastapausten välillä sekä annoslaskennan että isotoopin biologisten poistuma-aikojen suhteen.

Tutkimuksessa kehitettiin uusi annoslaskentamenetelmä ulkoiseen fotonisädehoitoon. Kehitetty *Pencil Beam* -pohjainen menetelmä sisältää uuden tiheydestä riippuvan tavan mallintaa epähomogeenistä väliainetta. Annoslaskennan tulokset vastaavat hyvin *Monte Carlo*-menetelmällä laskettuja tuloksia useissa eri tapauksissa. Havaitut erovaisuudet olivat pienempiä kuin 2% (tai 2 mm). Kehitetty menetelmä on laskennallisesti tehokas ja soveltuu hyvin annossuunnittelukäyttöön sädehoidossa.

Avainsanat sädehoito, annossuunnittelu, isotooppihoidot

ISBN (painettu) 978-952-60-6727-8 **ISBN (pdf)** 978-952-60-6728-5

ISSN-L 1799-4934 **ISSN (painettu)** 1799-4934 **ISSN (pdf)** 1799-4942

Julkaisupaikka Helsinki **Painopaikka** Helsinki **Vuosi** 2016

Sivumäärä 149 **urn** http://urn.fi/URN:ISBN:978-952-60-6728-5

Preface

This project started twenty years ago in the spring of 1996, when my Thesis advisors Kalevi Kairemo and Mikko Tenhunen recognized a need to improve treatment planning for radionuclide therapy. At the time, I was developing a treatment planning system for brachytherapy, and we started to extend the system to include radionuclide dose calculations. I am greatly indebted to my advisors for their support, creativity, and drive that pushed me to move this project forward. I also want express my gratitude to the patients presented in the case studies and the clinical staff involved in the patient care and data acquisition.

During my doctoral studies, I have been employed by Varian Medical Systems Finland Oy (formerly Varian-Dosetek Oy) working in radiotherapy research and development projects. I want to thank all my colleagues at Varian for the motivating and inspiring work environment where fighting against cancer is our common goal. Pekka Aalto created a world-class treatment planning research and development center at Dosetek in Finland, and supported me in many ways during the years. I am grateful to Ramin Baghaie for the support and encouragement that he gave me to finalize my doctoral studies, and for his perceptive review and comments on the manuscript.

I want to thank all the co-authors of the publications and my other collaborators. Jyrki Alakuijala has been an outstanding mentor inducting me to the process of scientific publication, as well as to the world of professional software development. The AAA method would not exist without Waldemar Ulmer's and Wolfgang Kaissl's early investigations and Hannu Helminen's key contributions during the first implementation. Since then, numerous people have contributed to the success of the AAA and its improvements: particularly the members of the VMS Finland Applied Research Department and the large user base of medical

physicists around the world.

At Aalto University, my sincere thanks go to Professor Toivo Katila, who guided me during the start of my doctoral studies, and to Professor Lauri Parkkonen who took over the supervision during the final stretch of my studies. I am grateful to the official pre-examiners, Professor Dietmar Georg and Dr. Mark Lubberink, for their insightful comments and appropriate suggestions. I want to express my gratitude to Raine Vasquez for his critical language review.

The encouragement and care from my parents Helena and Jorma has enabled my education and other endeavors in life. Thank you. Olavi and Ansa, you fill me with joy and keep me energized with your speed of movement and creativity. Finally Noora: without your love, companionship, exemplary passion for scientific writing and encouragement to finalize this undertaking, it would have taken me yet another twenty years.

Helsinki, March 22, 2016,

Joakim Pyyry

Contents

List of Publications

This thesis consists of an overview and of the following publications which are referred to in the text by their Roman numerals.

I J. Laitinen, J. Alakuijala, H. Helminen, S. Sallinen, M. Tenhunen, and K. Kairemo. Spect-based radioimmunotherapy planning system. In *IEEE Engineering in Medicine and Biology 19th Annual Conference*, Chicago, 781–784, 1997.

II J.O. Laitinen, K.J. Kairemo, A.P. Jekunen, T. Korppi-Tommola, and M. Tenhunen. The effect of three dimensional activity distribution on the dose planning of radioimmunotherapy for patients with advanced intraperitoneal pseudomyxoma. *Cancer* **80**, 2545–2552, 1997.

III J.O. Laitinen, M. Tenhunen, and K.J. Kairemo. Absorbed dose estimates for I-131 labelled monoclonal antibody therapy in patients with intraperitoneal pseudomyxoma. *Nucl Med Commun* **21**, 355–360, 2000.

IV J.O. Pyyry, J. Merenmies, M. Tenhunen, M. Heikinheimo, K. Parto, M. Arola,K. Rönnholm, H. Isoniemi, R. Karikoski, E.L. Kamarainen, M. Seppänen,J. Heikkonen, F. Augensen, W.H. Wegener, D.M. Goldenberg, and K.J. Kairemo . Radioimmunotherapy for recurrent childhood hepatoblastoma after liver transplantation. *World Journal of Nuclear Medicine* **7**, 146–157, 2008.

V W. Ulmer, J. Pyyry, and W. Kaissl. A 3D photon superposition/convolution algorithm and its foundation on results of Monte Carlo calculations.

Physics in Medicine and Biology **50**, 1767–1790, 2005.

VI L. Tillikainen, H. Helminen, T. Torsti, S. Siljamäki, J. Alakuijala, J. Pyyry, and W. Ulmer. A 3D pencil-beam-based superposition algorithm for photon dose calculation in heterogeneous media. *Physics in Medicine and Biology* **53**, 3821–3839, 2008.

Author's Contribution

Publication I: "Spect-based radioimmunotherapy planning system"

The author (J. Laitinen) implemented the dose-kernel-based dose calculation algorithm and dose visualization system and integrated the methods into an existing brachytherapy treatment planning system. The author was solely responsible of the production of the manuscript.

Publication II: "The effect of three dimensional activity distribution on the dose planning of radioimmunotherapy for patients with advanced intraperitoneal pseudomyxoma"

The author (J. Laitinen) developed and utilized a radiotherapy planning system to register images and calculate doses. The author analyzed the results and was primarily responsible of the writing and revision of manuscript.

Publication III: "Absorbed dose estimates for I-131 labelled monoclonal antibody therapy in patients with intraperitoneal pseudomyxoma"

The author (J. Laitinen) utilized the developed radiotherapy planning system and MIRD methodology to analyze radiation doses in patients receiving radioimmunotherapy. The author was primarily responsible of the production of the manuscript.

Publication IV: "Radioimmunotherapy for recurrent childhood hepatoblastoma after liver transplantation"

The author constructed the dose kernels for In-111 and Y-90 and analyzed the radiation doses utilizing the developed software employing automatic image registration and point-dose-kernel dose calculation. The author was jointly responsible for the production of the manuscript contributing to the absorbed dose calculation section and to the methods related to dose calculations and image registration.

Publication V: "A 3D photon superposition/convolution algorithm and its foundation on results of Monte Carlo calculations"

The author participated in developing the methods and verification of the implementation of the methods. The author analyzed the radiation doses utilizing the developed software and co-ordinated experimental verification of the methods. The author assisted in the production and review of the manuscript.

Publication VI: "A 3D pencil-beam-based superposition algorithm for photon dose calculation in heterogeneous media"

The author participated in developing the methods related to the exponential basis functions and scaling for tissue heterogeneities. The author had a minor role in assisting in the production and review of the manuscript. This article was also part of the PhD thesis of Tillikainen (2009).

Abbreviations and Symbols

A	Activity distribution
e	Electron radiation
E	Energy
Φ	Angular fluence
γ	Photon radiation
h	Pencil-beam dose kernel
k	Point-dose kernel
λ	Distance from the central axis
$\vec{p}$	Spatial position co-ordinate (p_x, p_y, p_z)
μ	Attenuation co-efficient
N	Number of elements
$\hat{\Omega}$	Direction
$\vec{r}$	Spatial position
ρ	Density
σ	Total cross section
S_R	Radiative stopping power
T	TERMA — Total energy released in the material
3D	Three dimensional
AAA	Analytical anisotropic algorithm
CAX	Central axis

CCC Collapsed cone convolution

CPU Central processing unit (of a computer)

CT Computed tomography

FFT (Discrete) fast Fourier transform

GPU Graphics processing unit

IMRT Intensity modulated radiotherapy

ICRU International commission on radiation units and measurements

MIRD Committee on medical internal radiation dose

MC Monte Carlo

MoAb Monoclonal antibody

MR Magnetic resonance

MSM Multiple source models

OLINDA Organ level internal dose assessment

PB Pencil beam

PET Positron emission tomography

QA Quality assurance

SBRT Stereotactic body radiation therapy

SC Superposition/convolution

S-factor Specific absorbed dose factor in MIRD methodology

SPECT Single-photon emission computed tomography

TERMA Total energy released in the material

TPS Treatment planning system

VMAT Volumetric modulated arc therapy

VOI Volume of interest

1. Introduction

Cancer is a malignant disease which is among the leading causes of mortality in the world, with approximately 14 million new cases annually in 2012 leading to 8.2 million deaths, according to World Health Organization. Cancer incidences rise with aging of the population, and it is estimated that there will be 70% more cancer cases within next two decades. (WHO 2015)

Cancer is a generic term for a group of diseases. The defining feature of cancer is the rapid growth of abnormal cells that spread to other organs by invading adjoining parts of the body or through circulation referred to as metastasizing. Metastases cause the majority of deaths from cancer.

Every cancer type requires a tailored approach to treatment. Treatment regimens include multiple modalities: surgery, radiotherapy, and chemotherapy. The different modalities are often used in combination. The goal of the treatment is to cure cancer or to prolong life, in addition to improving the patient's quality of life. Radiotherapy is a key component of comprehensive cancer care, but worldwide access to it is low. As Atun et al. (2015) point out there are considerable benefits to further develop radiotherapy and scale it up worldwide.

This Thesis explores and introduces improvements to computational methods that are used in the application of radiotherapy. These methods are routinely used in clinical radiotherapy practice and fall under the domain of computational physics. The methods are very relevant as they provide an optimal balance of accuracy and speed in the everyday practice of radiotherapy.

1.1 Principles of radiotherapy

Radiotherapy refers to the utilization of ionizing radiation for a therapeutic effect, typically for cancer treatment; for a comprehensive overview of the subject see e.g. Halperin et al. (2008). Radiation is delivered either externally, from outside the body, or internally. Internal therapy is further divided to brachytherapy and radionuclide therapy. In brachytherapy, a radioactive source is placed in or near the tumor; in radionuclide therapy, the radioactive isotopes are delivered systemically inside the body.

Ionizing radiation causes damage in cells, with increased damage by the amount of energy deposited by the ionizing radiation in the tissue. Both normal tissue and cancer cells are affected but exhibit different cell-survival probability for the same radiation dose level. Many cancer cells are more sensitive to radiation than healthy tissue due to the reduced efficacy of the biochemical repair processes of the damaged cell nuclei undergoing reproduction (due to the growth of the cancer). In addition, the ability to focus the radiation for a higher dose in the tumor compared to normal tissue allows for improved therapeutic ratio.

1.2 Brachytherapy

Brachytherapy is a form of radiotherapy where sealed radioactive sources are placed in the vicinity of the treated tumor. Typically it is applied internally via cavities or interstitially with needles. It is oldest form of radiotherapy as it was first applied in 1901 shortly after the discovery of radioactivity. Low dose rate delivery typically can involve permanent implants of sealed sources or temporary application of radioactive sources for several hours. Shorter high dose rate treatments are typically performed with afterloading devices where the radioactive source is moved in and out off the treatment region using remote control.

1.3 Radionuclide therapy

Radionuclide therapy is an internal radiotherapy technique which relies on certain biological mechanisms to provide a higher concentration of radionuclides in the vicinity of cancerous cells in order to produce a higher radiation dose. Often radionuclide therapy relies on radiolabeled carriers like liposomes, antibodies, or nano-particles to localize in tumors

(Williams et al. 2008). The radionuclides are administered systemically via circulation, or into cavities.

The radionuclides that are useful for therapy undergo three modes of decay: beta, alpha, and electron capture or isomeric transition by emission of Auger and Coster-Kronig electrons. Selection criteria, in addition to the mode of decay, include energy of released particles, chemical properties, production methods, as well as biological behavior (Zweit 1996).

Similarly to other modes of radiotherapy — knowledge of the absorbed radiation dose is needed to assess the toxicity and efficacy of radionuclide therapy. The absorbed dose is a macroscopic concept, but for radionuclide therapy microdosimetry — study of radiation energy deposition in microscopic volumes — may be indicated for low-energy auger-emitters (Humm et al. 1993). The notion of biological effective dose has been introduced to take into account the biological effects various dose rates and different types of radiation. The aspects of radiobiology can be utilized in radionuclide therapy in order to estimate the best dose for tumor control, while protecting the healthy tissues (Pouget et al. 2015).

1.4 External-beam radiotherapy

External-beam radiotherapy is a mode of radiation treatment where the radiation originates from sources externalto the body. The radiation types used are photons, electrons, or heavier charged particles. The most common is photon therapy using megavoltage brehmsstrahlung x-rays generated by linear electron accelerators. Photon beams can also be generated with a radioactive source such as cobalt-60. Charged-particle therapy has its own role in cancer management but is not discussed in the Thesis.

The external beam is directed from outside the body to the site of the treatment target (tumor). In order to ensure a conformal and high radiation dose inside the target, the radiation needs to be focused from multiple directions to the common target. The beam intensity and shape are typically produced by a computer-controlled multi-leaf collimation device integral to the treatment delivery system.

1.5 Radiation physics of photons and electrons

Photon radiation interacts with matter and deposits energy via complex interaction cascades. When photons interact with material, the primary photon is absorbed in the interaction. A secondary photon is re-emitted in a scattering (coherent or incoherent) interaction. The scattering process is similar to a change in the direction and energy of the photon; this change occurs through absorption and emission of photons. In the process, electrons are also ejected from the interacting atoms or they are created as electron — positron pairs. The main interactions of photons with atoms are called photoelectric absorption, Rayleigh (coherent) scattering, Compton (incoherent) scattering, and electron — positron pair production. The relative importance of various interactions varies with photon energy and the medium. The total mass attenuation coeffiecients have been tabulated extensively by Hubbell and Seltzer (1996) and Figure 1.1 shows an example of photon attenuation factors as function energy.

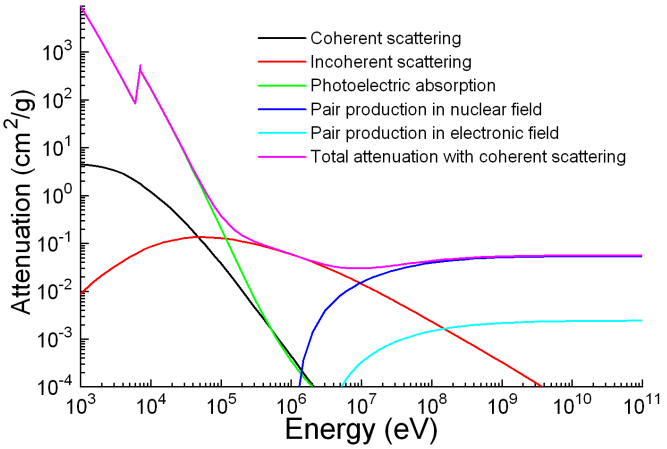

Figure 1.1. Photon attenuation is plotted separately for each interaction type with the total mass attenuation factor as a function of energy in iron medium (Tuszynski 2010).

In photon radiotherapy, electrons are generated in the interactions of the photons with matter. These electrons interact intensively with matter. Electrons interacting with the orbital electrons of the atoms create secondary electrons and lose part of their initial energy. Photons are created when the electrons interact with the Coloumb field of the nucleus of the atom in a process called brehmsstrahlung. The electromagnetic interactions couple the electrons and photons into a combined shower of particles which makes the modeling of the phenomenon complicated.

1.6 Radiation transport and absorbed dose calculations

The radiation transport problem can be described as a linear differential equation that takes the form of the Boltzmann transport equation originally formulated by Ludwig Boltzmann to describe the statistical behavior of a thermodynamic system not in a thermodynamic equilibrium. The transport equation can be solved by numerical grid-based methods, as has been demonstrated in the radiotherapy domain by several groups (Kotiluoto et al. 2007; Vassiliev et al. 2010). However, the historically more important method in the field of radiotherapy has been the stochastic Monte Carlo (MC) solution to the Boltzmann transport equation (Andreo 1991; Rogers 2006). There have been several practical implementations where speed and accuracy have been optimized for routine clinical use (Neuenschwander et al. 1995; Fippel et al. 1997; Fippel et al. 1999; Kawrakow and Fippel 2000; Fix et al. 2010).

The Boltzmann equation for transport of photons (γ) can be written as

$$\hat{\Omega} \cdot \vec{\nabla}\Phi^{\gamma} + \sigma_t^{\gamma}\Phi^{\gamma} = q^{\gamma} + q^{\gamma\gamma} \tag{1.1}$$

and for electrons (e) the Boltzmann-Fokker-Planck transport equation as

$$\hat{\Omega} \cdot \vec{\nabla}\Phi^{e} + \sigma_t^{e}\Phi^{e} - \frac{\partial}{\partial E}(S_R\Phi^{e}) = q^{e} + q^{ee} + q^{\gamma e} \tag{1.2}$$

where $\Phi(\vec{r}, E, \hat{\Omega})$ describes the angular fluence for photons and electrons and is a function of spatial position ($\vec{r}$), energy (E) and direction ($\hat{\Omega}$). The macroscopic total cross sections for photons is σ_t^{γ} and for electrons σ_t^{e}. $S_R(\vec{r}, E)$ is the combined restricted collisional and radiative stopping power. The scattering source terms can be written in the integral form as

$$q^{\gamma\gamma}(\vec{r}, E, \hat{\Omega}) = \int_0^{\infty} dE' \int_{4\pi} \sigma_t^{\gamma\gamma}(\vec{r}, E' \rightarrow E, \hat{\Omega} \cdot \hat{\Omega}')\Phi(\vec{r}, E, \hat{\Omega}) d\hat{\Omega}' \tag{1.3}$$

$$q^{\gamma e}(\vec{r}, E, \hat{\Omega}) = \int_0^{\infty} dE' \int_{4\pi} \sigma_t^{\gamma e}(\vec{r}, E' \rightarrow E, \hat{\Omega} \cdot \hat{\Omega}')\Phi(\vec{r}, E, \hat{\Omega}) d\hat{\Omega}' \tag{1.4}$$

$$q^{ee}(\vec{r}, E, \hat{\Omega}) = \int_0^{\infty} dE' \int_{4\pi} \sigma_t^{ee}(\vec{r}, E' \rightarrow E, \hat{\Omega} \cdot \hat{\Omega}')e(\vec{r}, E, \hat{\Omega}) d\hat{\Omega}', \tag{1.5}$$

where $q^{\gamma\gamma}$ is the photon source resulting from photon interactions, $q^{\gamma e}$ is the electron source resulting from photon interactions and q^{ee} is the electron source resulting from electron interactions. The corresponding macroscopic differential cross sections are $\sigma_t^{\gamma\gamma}, \sigma_t^{\gamma e}, \sigma_t^{ee}$ for photon–photon, photon–electron, and electron–electron interactions respectively. The

above equations are somewhat simplified in the interactions such that photons can produce electrons but electrons do not produce photons. Additionally, the pair-production particles are assumed to be electrons (instead of an electron–positron pair). Additionally, the electrons are transported with a continuous slowing down approximation. In the radiotherapy domain, these simplifications are not affecting the accuracy of the solution (Vassiliev et al. 2010).

The solution of the transport equation allows for an accurate determination of the absorbed energy in the material including the relevant physics. As reviewed earlier, photons are indirectly ionizing particles and do not deposit significant energy, but through interaction with medium they transfer their energy to electrons and positrons that ionize and transfer their energy until it is exhausted. The energy absorbed can be further converted into absorbed dose which is strictly defined as mean energy imparted (by ionizing radiation) per mass (ICRU 1988).

In this Thesis methods that directly solve the transport equation are not utilized but rather other methods to calculate the absorbed dose are employed. These methods are typically phenomenological models or mathematical constructs that separate the effects of scattered radiation from the primary radiation such as the Superposition/convolution (SC) algorithm and are reviewed further in Chapter 3.

1.7 Aims of the Thesis

The aims of this Thesis are summarized in the Table 1.1 below. The methods developed in this Thesis are to provide the basis for accurate and fast absorbed dose calculations in the external-beam radiotherapy and radionuclide therapy, and are to be applied in analysis of radionuclide treatments.

Table 1.1. Aims of the Thesis

Aim	**Publication**
1. To develop a general methodology for three dimensional (3D) treatment planning of radionuclide therapy	I, II
2. To apply convolution (dose-kernel) methods in radionuclide therapy treatment planning in order to compare a patient-specific dose calculation method with the widely used Committee on medical internal radiation dose (MIRD) S-factor model for patients receiving radionuclide therapy.	II, III, IV
3. To develop a Pencil-beam (PB) dose-kernel-based calculation method for external photon therapy that also accounts for local variations in tissue material densities in 3D space.	V, VI

2. Radiotherapy treatment planning and sources of radiation

The overall radiotherapy treatment planning process aims to model the treatment outcome. Current practice is to calculate and analyze radiation dose as a surrogate for biological effectiveness of the treatment. The overall process is depicted in Figure 2.1. The process is similar for radionuclide and external-beam therapy. The main difference is the patient-specific radionuclide imaging that is used to construct the radiation source model in radionuclide therapy, whereas in external-beam therapy the source modeling is independent of the patient.

The treatment planning process starts with acquisition of anatomical images used for anatomy modeling and dose calculation. X-ray Computed tomography (CT) is suitable for dose calculation purposes due to its geometrical accuracy and ability to provide density and material composition data. Magnetic resonance (MR) imaging provides great soft tissue contrast and is very useful for determining the boundaries of critical organs and extent of macroscopic tumor growth. Anatomy modeling is done by manually or semi-automatically segmenting the image data, providing geometrical models of the patient's anatomy. Dose calculation uses the source model and an algorithm to solve the radiation transport problem in the patient-specific geometry. The resulting dose distribution is visualized and analyzed utilizing e.g. dose volume histograms (Drzymala et al. 1991). A computer implementation of the radiotherapy process and methods is called a Treatment planning system (TPS).

2.1 Dose calculation in radionuclide therapy

The absorbed dose in radionuclide therapy has commonly been calculated using biokinetic data from a diagnostic tracer study, using a method developed by the MIRD (Watson et al. 1993). The traditional MIRD method

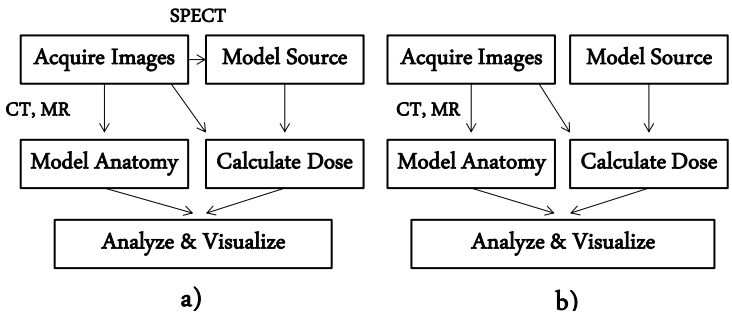

Figure 2.1. The treatment planning process for a) radionuclide therapy and b) external-beam radiotherapy are very similar.

includes a model patient phantom where various organ-to-organ contributions of dose have been pre-calculated with the MC method to solve the above transport equations. When applied in a clinical setting, the MIRD method fails to include patient-specific anatomy and non-homogenous distribution of the radionuclide inside a given organ. A computer implementation of the methodology that is currently widely used is called Organ level internal dose assessment (OLINDA) (Stabin et al. 2005).

Various authors have studied methods that overcome these limitations. Although Traino et al. (2013) report on a simplified patient-specific method based on the MIRD S-factors, the most common solution is to calculate the absorbed dose distributions using a point-source-kernel approach with patient-specific activity maps (Sgouros et al. 1990; Sgouros et al. 1993; Erdi et al. 1994; Kolbert et al. 1997; Giap et al. 1995b; Giap et al. 1995a; Erdi et al. 1998; Gardin et al. 2003; Guy et al. 2003; Loudos et al. 2009). This method is also utilized in papers I, II, III and IV. Another approach is to utilize the so called voxel S-factors to calculate patient-specific dose estimates in combination with point kernels as described by Jackson et al. (2013). As in external-beam radiotherapy, MC calculations have also been proposed and applied in radionuclide therapy for patient-specific dose calculations by Tagesson et al. (1996) and Furhang et al. (1996a) and Furhang et al. (1997) and more recently applied e.g. by Ljungberg et al. (2002), Chiavassa et al. (2005), Prideaux et al. (2007), Marcatili et al. (2013), and Grimes and Celler (2014). Dieudonné et al. (2013) has compared accuracy between the dose kernel methods and MC methods.

2.2 Distribution of activity in radionuclide therapy

Overall treatment planning and dosimetry of radionuclide therapy requires an estimation of the radionuclide activity distribution in the patient over time (Strand et al. 1993b; Sgouros et al. 1990). This cumulative activity distribution can be derived form nuclear medical imaging techniques (planar gamma camera, Positron emission tomography (PET), and Single-photon emission computed tomography (SPECT)) and pharmacokinetic data. The image data has to be quantified so that absolute activity counts needed for cumulative activity distribution can be obtained. Additionally, pharmacokinetic modeling complements the estimation of cumulated activity in the image. The basic pharmacokinetic modeling of radiolabeled Monoclonal antibody (MoAb) has been reviewed by Strand et al. (1993a) and a software package to calculate cumulated activities has recently been developed by Kletting et al. (2013).

The general goal for emission-computed tomography is to be able to quantitatively determine localization volumes and measurement of activities in small and large tumors. There are various factors that affect the accuracy of the quantification of emission-computed images. In SPECT, the most important physical factors are scatter and attenuation corrections, limited spatial and energy resolutions of gamma cameras, septal penetration of high energy photons, and statistical noise of low count densities. The system resolution is about 9 mm and full-width-at-half-maximum of SPECT devices range from 7 - 18 mm, which leads to partial volume effects i.e. loss of apparent activity within small objects (Erlandsson et al. 2012). The use of PET would provide improved spatial resolution and quantification. For PET systems, the spatial resolution is about 6 - 13 mm. The limitations of PET has been the availability of the technology and problems associated with short lived radionuclides. Lubberink et al. (1999) and Lundqvist et al. (1999) discuss the use of PET for radionuclide quantification and dosimetry.

For treatment planning purposes, the imaging can be done prior to therapy or during therapy to verify estimate actual dose delivered, and both methods where used in II, III and IV. The pre-therapy imaging can be carried out using an appropriate radionuclide label for the targeting agent with a gamma camera or positron camera. The pre-therapy forms the basis of targeted radionuclide therapy planning. Therapy imaging is more demanding but is essential for confirming the information provided

by pre-therapy planning study.

The information that is crucial to dosimetry is tracer concentration at several time points throughout the residence time of the tracer. The images need to be corrected for detector uniformity of response and dead-time, photon attenuation and scattering effects (Ott 1996). The conversion of image data in counts per voxel to concentration requires calibration data of phantoms imaged with known radioactive concentration of tracer. The accuracy of the kinetics of the radionuclide concentration is furthermore restricted by the temporal sparseness imaging data.

The kinetics of the therapeutic dose may vary from the tracer dose. Although the pre-therapy dosimetry is important in the guidance of the treatment, the actual dose delivered in treatment needs to be determined using on-therapy imaging. The estimation of doses in III and IV where done based on on-therapy SPECT images and quantification using planar gamma camera images with a standard source as a reference.

Obtaining qualitative data of activity distributions from SPECT requires careful methods in acquiring and processing the data (Ott 1996; Leichner et al. 1993; Dewaraja et al. 2012). Quantitative planar and SPECT images can be obtained by using attenuation and scatter correction methods. Hutton et al. (2011) have produced a recent review of the current scatter correction methods and notes that the most widely used ones are the scatter subtraction by multiple energy window approaches, as described by Macey et al. (1995). Ljungberg et al. (1994) have compared a few different methods and concluded that there is no significant difference in quantification accuracy between them.

Improved reconstruction accuracy using iterative methods is an active research area (see e.g. (Beekman et al. 2002; Ouyang et al. 2007)). An application of such methods in radionuclide therapy with absorbed dose estimation has been reported by Cheng et al. (2014). The emerging hybrid SPECT/CT and PET/CT devices are also aiding in better reconstruction and image processing methods for quantitative imaging by providing complementary information about the attenuation properties of the patient (Cade et al. 2013). It is essential to validate the methodology used to extract quantitative information from reconstructed images because different devices and reconstruction algorithms have a big effect on the quality of the images.

2.3 Treatment machine modeling

In order to characterize the energy fluence output of a linear accelerator suitable for transport equation solvers or model-based SC and Pencil beam (PB) algorithms, one needs a physical source model of the treatment machine. The output of a treatment machine is well understood thanks to the extensive study of radiation output based on the geometrical construction (of the machine) by utilizing the MC method — see e.g. Mohan et al. (1985), Ma et al. (1999), Sheikh-Bagheri and Rogers (2002b) and Sheikh-Bagheri and Rogers (2002a) using MC based tools like BEAM as described by Rogers et al. (1995).

For practical application, simplified models have been developed that divide the main sources of radiation into several components that can be described by a small set of model parameters. These are called Multiple source models (MSM) and have been developed by various independent researchers like Liu et al. (1997), Fix et al. (2001b), Deng et al. (2004), Fippel et al. (2003), Fix et al. (2004), and Tillikainen et al. (2007) for the purposes of dose calculations. Another use for simplified source models is in Quality assurance (QA), where independent monitor unit calculations can be performed with simplified energy fluence models (Georg et al. 2007).

Typical MSM models include a point source for primary radiation from the bremsstrahlung target and finite size sources to account for extrafocal radiation from flattening filter, primary collimators, and secondary jaws. The models also include treatment of the electrons escaping the linear accelerator in addition to the photon sources. Figure 2.2 shows schematically a two source photon model with the target and flattening filter showing in red as the effective photon sources; in addition, electrons are generated in air by the photon radiation. Some of the models are derived from MC simulation data tuned to match a given linear accelerator, which is a very time consuming process (Ojala 2014). A more practical approach is to fit model parameters to a set of measurements for a given treatment unit in an automated fashion as described by Tillikainen et al. (2007).

Various photon beam dose models are reported to reproduce dose calculation results in water within 1-2% accuracy (Jiang et al. 2001; Fix et al. 2001a). Ahnesjö et al. (2005) report the performance of their MSM for a large number of clinical linear accelerators in which 87% machines can

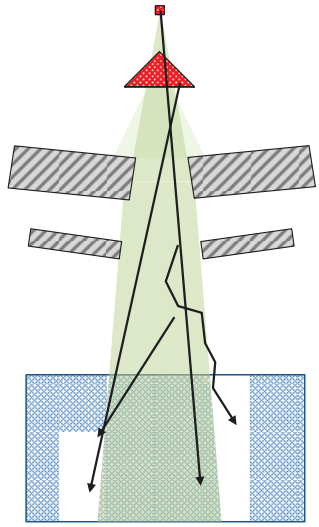

Figure 2.2. A schematic drawing of a medical linear accelerator as the radiation source in external-beam radiotherapy.

be modeled within 2.5% maximum error. The final element of the modeling of the output of a linear accelerator is the back-scatter to the monitor chamber (Verhaegen et al. 2000; Jiang et al. 2001). The back scatter effect can be included as a correction factor or as a more comprehensive model like that described by Liu et al. (2000). The overall accuracy of dose calculation approach determined both by the accuracy of the source model and the radiation transport in the patient geometry is discussed in the next section.

3. Model-based convolution and superposition methods in absorbed dose calculation

3.1 Background

Widely used model-based dose calculation methods are SC and PB algorithms. The models in these algorithms separate the handling of the primary photons from the scattered photons, and later combine the effects of scattered radiation by distributing this in a large volume. The underlying physics can be utilized to calculate the model parameters, or the parameters can be obtained by fitting the model to measurements. Although both algorithms separate the primary radiation from the scattered radiation, they differ in how the separation is done.

In the SC method, the scatter is modeled as a point-spread kernel — as a Three dimensional (3D) kernel for a given point in the interacting matter — whereas, in the PB method, the scatter is modeled as a planar (2D) depth-dependent kernel that is distributed perpendicularly to the ray lines of the primary radiation from a external point source. Figure 3.1 illustrates the different view points of the a) PB and b) SC algorithms. The PB method views dose deposited from a small narrow beam with a varying shape at each depth that includes all effects from upstream scattering events and utilizes this to compose broad beam distributions. The SC method looks at an unidirectionally moving single photon always interacting at the same point and producing a point-dose-spread kernel that is used in an macroscopic situation.

The case c) shows kernel of radiation dose of a single point source which is utilized for internal radiotherapy (brachytherapy or radionuclide therapy), where radiation can be modeled as point sources inside the Volume of interest (VOI). This method is different from the two others as no separation of scattered dose is attempted, rather the dose kernel includes all

effects of a single point source depositing dose by interactions with the matter.

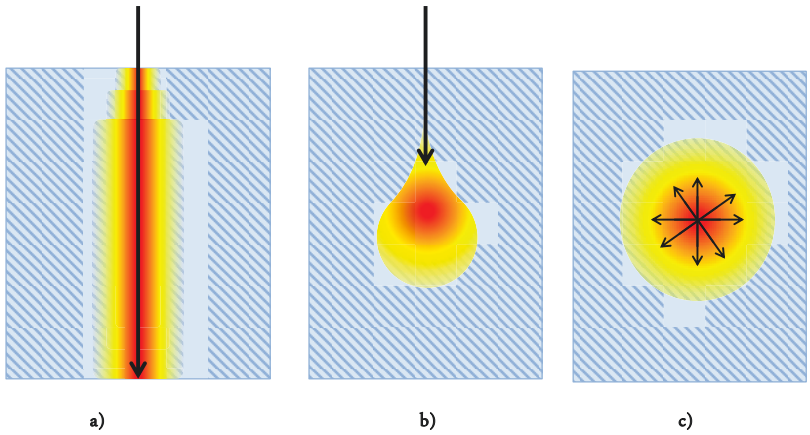

Figure 3.1. Different kernel-based methods have different geometrical separation of the source term (primary) and the scattered radiation dose. The kernels from left to right a) PB kernel b) a point-spread kernel and c) point source dose kernel.

3.2 Point-spread and kernel methods

3.2.1 Brachytherapy

The most widely used method to calculate absorbed dose around brachytherapy sources are based on the formalism and data from the AAPM Task Group 43 recommendations (Rivard et al. 2004; Nath et al. 1995). The method allows inclusion of the effects of the anisotropic distribution around linear sealed radioactive sources. The method provides absorbed dose distribution in water medium. The effect of medium heterogeneity can be included using transport equation solvers (Poon et al. 2008; Zourari et al. 2010; Lemaréchal et al. 2015) or by applying the SC method for brachytherapy as investigated by Carlsson and Ahnesjö (2000b) and Carlsson and Ahnesjö (2000a). The more accurate methods are especially useful in the context of improving dose calculation results in the presence of radiation shields (Tedgren and Ahnesjö 2003; Petrokokkinos et al. 2011).

3.2.2 Radionuclide therapy

As discussed earlier, the point-source-kernel approach can provide patient-specific dose calculations in radionuclide therapy by using an activity map of the distribution of the radionuclide as input. Absorbed dose distribution $D(\vec{r})$ at point $\vec{r}$ of known cumulative activity distribution $\tilde{A}(\vec{r})$ in a homogenous medium can be calculated with a convolution integral (Giap et al. 1995b):

$$D(\vec{r}) = \int_{V'} \tilde{A}(\vec{r}\,')k(|\vec{r} - \vec{r}\,'|)dV', \tag{3.1}$$

where $k(r)$ is a point source dose kernel (i.e. a spherically symmetric dose distribution of point source of unit cumulative activity, see 3.1 c)). The kernels can be obtained from MC simulations, analytical calculations, or physical measurements. Dose kernels have been constructed using the MC method, for instance by Furhang et al. (1996b) and Reiner et al. (2009), or from cross sectional material data by Leichner (1994).

The convolution integral is effectively computed discretely using the (Discrete) fast Fourier transform (FFT) as investigated by various authors, both in the realm of brachytherapy and radionuclide therapy dose calculations (Boyer and Mok 1986a; Giap et al. 1995b). The 3D kernel and the 3D activity map are transformed into the Fourier space, where the convolution is calculated by multiplication and transformed back to the spatial domain using an inverse FFT providing the solution to the convolution integral.

3.2.3 3D kernel methods in external-beam therapy

As discussed earlier, in external-beam therapy the 3D dose kernel has a different meaning compared to internal therapy. Here, the 3D kernel is a cumulative dose-spread array of photons interacting in a single point in the medium. It includes all the effects of photon and electron scatter interactions leading to adsorbed energy (radiation dose) in the medium. These dose-spread arrays can be calculated and tabulated by using the MC method, see Mackie et al. (1988).

The kernel methods rely on the fact that the broad beam dose can be composed of multiple point irradiations that cause a response that can be summed up over the whole problem (superposition). The attenuation of incident photons interacting in the medium is calculated and the Total energy released in the material (TERMA) is determined. The transport of energy by scattered photons and electrons is described by the point-spread

kernel. The dose distribution is the superposition of the kernels, weighted by the magnitude of the TERMA impulse for all interaction sites. These methods were actively developed for the radiotherapy treatment planning calculations in mid 1980s by several independent groups, as reported by Mackie et al. (1985), Boyer and Mok (1986b), Boyer and Mok (1985), and Boyer et al. (1989), Mohan and Chui (1987) and Ahnesjö et al. (1987).

In the most simplest geometries (homogenous materials and simplified source models), the kernels are spatially invariant, making the superposition a convolution integral similar to Equation 3.1 where the activity term $\tilde{A}(\vec{r}\,')$ is replaced by TERMA $T(\vec{r}\,')$. In this case, this can be very effieciently computed with the FFT method and was studied by various authors like Boyer and Mok (1985), Boyer et al. (1989), and Mohan and Chui (1987). Boyer (1984) and Boyer and Mok (1986b) have extended the methods for heterogeneous materials by separating kernels into single and multiple scattering events and applying first order approximations. The basis of the approximations were developed further by Wong et al. (1996). The more elaborate treatment of heterogeneity is to scale kernels by ray-tracing methods, which has become the more prevalent method. A computationally effective method for the density-scaling is to utilize spatial discretization of the scattering angle and parametrization of scatter kernels with exponential basis functions, as employed by Ahnesjö (1989) in his Collapsed cone convolution (CCC) algorithm.

3.3 Pencil-beam methods

The specifics of PB methods as described in VI and V are summarized in this section. The overview here is compressed and more details can be found in the original papers. The algorithm has also been commercially released as the Analytical anisotropic algorithm (AAA) in Eclipse^{TM} TPS. The heterogeneity correction applied in this method is also analogous to ray-tracing methods used in the 3D SC algorithms.

A PB kernel is a function produced by a narrow beam of monoenergetic photons of energy E, impinging on a semi-infinite perpendicular water phantom as depicted in Figure 3.1 a). The polyenergetic PB kernel function is $h_\beta(z,r)$, where z and r represent the distance from the surface and the orthogonal distance from the central axis, respectively. The kernels $h_\beta(z,r)$ can been obtained from MC simulations (Ahnesjö et al. 1992) or deconvolutions from measurements, as described by Storchi and Woud-

stra (1996) and Storchi et al. (1999).

3.3.1 Exponential modeling of pencil beams

The methods described in V and VI assume that the pencil beam can be separated into depth-directed and lateral components. The depth-directed component accounts for the total energy deposited by the pencil beam for each layer p_z in the calculation grid:

$$I_\beta(p_z) = \Phi_\beta \iint h_\beta(t, \upsilon, p_z)\, \mathrm{d}t\, \mathrm{d}\upsilon, \tag{3.2}$$

where Φ_β is the primary energy fluence for the beamlet β.

Lateral dose deposition is modeled as a sum of N radial exponential functions both in VI and Ahnesjö et al. (1992), whereas in V the lateral shape is modeled as Gaussian functions. The kernel is separated into sectors at angle θ as the fraction of energy deposited onto an infinitesimally small angular sector at distance λ from the beamlet central axis. The angular sectors allow for the heterogeneity correction in the lateral direction by ray-tracing along the discrete rays that represent the collapsed sectors. Given a number N of exponential function components (defined by coefficients μ_i), the exponential representation of the lateral pencil-beam component for a given depth plane p_z is of the form

$$k_\beta(\theta, \lambda, p_z) = \sum_{i=1}^{N} c_i(\theta, p_z) \frac{1}{\mu_i} e^{-\mu_i \lambda}, \tag{3.3}$$

where the attenuation coefficients μ_i are the same for all planes to allow an efficient computer implementation. The weight parameters $c_i(\theta, p_z)$ are fitted to the underlying PB kernel data obtained from MC simulations. The parameter N is chosen to balance between speed and accuracy, and in the implementation in VI we use the value $N = 6$.

3.3.2 Superposition of pencil beams

In a homogeneous water, the energy $E_\beta(\vec{p})$ deposited from a pencil-beam beamlet β into a point $\vec{p}$ is the product of the energy deposited on the calculation plane (I_β) and the corresponding lateral scatter kernel (k_β). A factor of $1/\lambda$ is also included for normalization:

$$E_\beta(\vec{p}) = I_\beta(p_z) \frac{1}{\lambda} k_\beta(\theta, \lambda, p_z), \tag{3.4}$$

To account for heterogenous material, the density-scaling approximation where each spatial dimension of the scatter process is scaled locally

by the inverse relative electron density $1/\rho_{\mathrm{w}}$ can be used:

$$\rho_{\mathrm{w}}(\vec{p}) := \rho^{\mathrm{elec}}(\vec{p})/\rho^{\mathrm{elec}}_{\mathrm{water}}, \tag{3.5}$$

where ρ^{elec} is the local electron density at point $\vec{p}$ and $\rho^{\mathrm{elec}}_{\mathrm{water}}$ the electron density of water. It is necessary to account for the effective (radiological) distance $d_{\mathrm{eff}}(X) = \int_X \rho_{\mathrm{w}}(\vec{p})\mathrm{d}\vec{p}$ for an arbitrary path X.

The scaling of the lateral scatter kernel is done by calculating the radiological path length in a radial manner from the center of the pencil beam. Then the heterogeneity-corrected lateral kernel $k'_\beta(\theta, \lambda, p_z)$ is given by

$$k'_\beta(\theta, \lambda, p_z) = k_\beta(\theta, \frac{p'_z}{p_z}\lambda', p'_z)\rho_{\mathrm{w}}(\vec{p}), \tag{3.6}$$

where λ' is the effective radius computed as $\lambda' = d_{\mathrm{eff}}(C_\beta(\theta, p_z))$. This radiological pathlength scaling method based on electron density is a common approach to account for tissue heterogeneities in kernel based models, as reported in the review by Ahnesjö and Aspradakis (1999), and has been found to be more appropriate than the scaling based on mass density by Seco and Evans (2006).

The I function also needs to be scaled for heterogeneities by expressing it in terms of effective depth p'_z. Thus, the heterogeneity corrected depth-directed component I'_β is calculated as

$$I'_\beta(p_z) = I_\beta(p'_z)\rho_{\mathrm{w}}(\vec{p_\beta}), \tag{3.7}$$

where $\vec{p_\beta}$ is the point on the pencil-beam central axis at depth p_z, p'_z is the effective depth given by $d_{\mathrm{eff}}(P_\beta)$, where P_β is the path from pencil-beam entry point to $\vec{p_\beta}$.

The heterogeneity-corrected energy distribution from a single beamlet β is then calculated as:

$$E_\beta(\vec{p}) = I'_\beta(p_z)\frac{1}{\lambda}k'_\beta(\theta, \lambda, p_z). \tag{3.8}$$

The total deposited energy into a grid point $\vec{p}$ is then simply an integral of contribution of all the individual beamlets over the broad beam area:

$$E_{\mathrm{tot}}(\vec{p}) = \iint_{\beta'} E_{\beta'}(\vec{p})\ \mathrm{d}\beta'. \tag{3.9}$$

3.3.3 Build-up and build-down correction

The separation of the heterogeneity correction into two components, the depth-directed component in (3.7) and the lateral scatter component in

(3.6) is clearly an approximation, but it produces good results after sufficient distance from the material interface in slab-like phantoms. However, near the interfaces it fails to reproduce the gradual build-up and build-down effects — instead, the dose would jump abruptly to a new equilibrium level. This is caused by the fact that the scattered particles originating before the interface are not correctly taken into account by this method.

The size of the build-up or build-down transition is determined by the mean range of the scattered particles. Also, the dominant scatter component in a therapeutic radiation beam is forward-directed. Thus to reproduce these effects using a pencil-beam based model, it is not sufficient to scale the pencil beam in its entirety by the effective distance, but a method to account for the forward-directed energy shift is needed.

The technique chosen in this work is to employ a forward build-up convolution kernel to the energy deposition introduced in V and refined in VI using a build-up kernel k_{b}. The convolution is done with the energy density distribution in terms of effective distance in the following way:

$$E_{\mathrm{b}}(\vec{p}) = \int_{t=0}^{p_z} E_{\mathrm{tot}}(p_x, p_y, t) k_{\mathrm{b}}(d_{\mathrm{eff}}) \rho_{\mathrm{w}}(p_x, p_y, t) \mathrm{d}t, \tag{3.10}$$

where d_{eff} is the (signed) effective distance from (p_x, p_y, p_z) to (p_x, p_y, t), and the multiplication with ρ_{w} is due to the change of variables from effective depth to true depth. This correction effectively shifts energy deeper, so the original pencil beams would no longer be accurately reproduced. For example, the original build-up at the surface of the pencil beam would be further stretched. Hence, it is necessary to pre-compensate in the I function in (3.2) using a deconvolution approach.

3.4 Computational considerations

3.4.1 Performance characteristics

In this section, computational complexity of various SC algorithms is reviewed. For the purpose of the analysis, a 3D calculation grid $N \times N \times N$ will be considered with M number of rays for ray-tracing for scatter scaling and G is the number of energy groups. The Table 3.1 contains the computational complexities of the various dose calculation algorithms.

An example of running time of a computer implementation of the PB method in VI is about 10 s for a 40×40 mm^2 field and about 60 s for a

Table 3.1. Computational complexity of different dose deposition algorithms

Algorithm	**Complexity**
Discrete convolution	N^6
Discrete FFT convolution	$kN^3 \log N^3$
Ray-traced scaled 3D SC	N^7
CCC	MN^4
AAA^{TM}	MN^3
AcurosXB^{TM} (Deterministic Transport Solver)	GMN^3

400×400 mm^2 field, respectively (on a dual-core Intel Xeon 5160 platform with 8 GB of memory and two processors).

3.4.2 Parallel computing

The performance of computers has increased dramatically during the lifetime of semiconductor based computing. The improvements were mainly driven by improving clock speed and larger and faster memory access. The increase in speed using these methods is, however, at its limit due to energy consumption and heat emission of processing chips as well as other physical limitations. In recent years, parallel computing has emerged as an alternative approach to further boost performance.

Central processing unit (of a computer) (CPU) of computers currently have multiple processor cores to allow for parallelism. Another manifestation of the parallel computing architecture is a Graphics processing unit (GPU). The GPU has evolved from its origin in computer graphics and visualization to a general purpose parallel computing device. Computationally challenging scientific problems have been widely solved using GPU technology in recent years. It has also been successfully employed in the radiotherapy domain. The various radiotherapy applications of GPU technology have been reviewed by Pratx and Xing (2011) and Jia et al. (2014).

The radiation dose calculation methods can be formulated in such a way that data parallel implementations on GPU platforms are possible. This has been an active area of research in the past few years. Jia et al. (2011) have implemented MC calculation method in GPU and report almost two orders of magnitude speed up compared to CPU based computation. Hissoiny et al. (2009), Hissoiny et al. (2010), Jacques et al. (2011), and Chen et al. (2012) report of GPU implementations of the SC method.

Additionally, Chen et al. (2011) report an extremely efficient implementation of the CCC algorithm, where calculation times can be pushed below 1 s per beam for a grid of 256^3 calculation points on modern GPU platforms (NVIDIA GTX295). Gu et al. (2009) has applied GPU technology to successfully implement an ultra-fast dose calculation engine using the PB method. These developments open up new opportunities for interactive dose shaping tools and more accurate solutions to the inverse problems in radiotherapy treatment planning.

4. Summary of results

4.1 Patient-specific distributions in radionuclide therapy

The first aim for this research was to produce a dose planning system for radioimmunotherapy by leveraging an existing radiotherapy treatment planning system and implementing a faster dose kernel convolution algorithm. The aim was also to develop novel 3D absorbed dose visualization methods. The results reported in I were a successful implementation of a radionuclide therapy planning system utilizing a fast point dose kernel calculation method and expanding visualization and user interface of the existing radiotherapy TPS. The developed system was used to analyze variability of biological uptake and clearance of the therapy agent in various patients and to estimate absorbed doses based on a point dose kernel dose calculation method in II. The main results were that both the inter-patient variability of biological clearance and localized differences for individual patients warrant the use of serial SPECT imaging to be able to determine patient-specific absorbed doses.

The clearance times for two different patients are plotted in Figure 1 of II. The clearance is assumed to contain two exponential components, thus the biological half-lives was calculated for both components. The exponential trend for the clearance determined from the SPECT images is also shown in the same figure. Spatial variation of the activity clearance was analyzed in the intra-therapeutic SPECT images by dividing the images into sub-volumes 64 cm3 (4 x 4 x 4 cm). The biological half-lives and clearance times of for each of these sub-volumes were calculated and the results are summarized in Table 1 (II). Additionally, patient absorbed doses were calculated based on cumulated activity and the activity map from the first SPECT study.

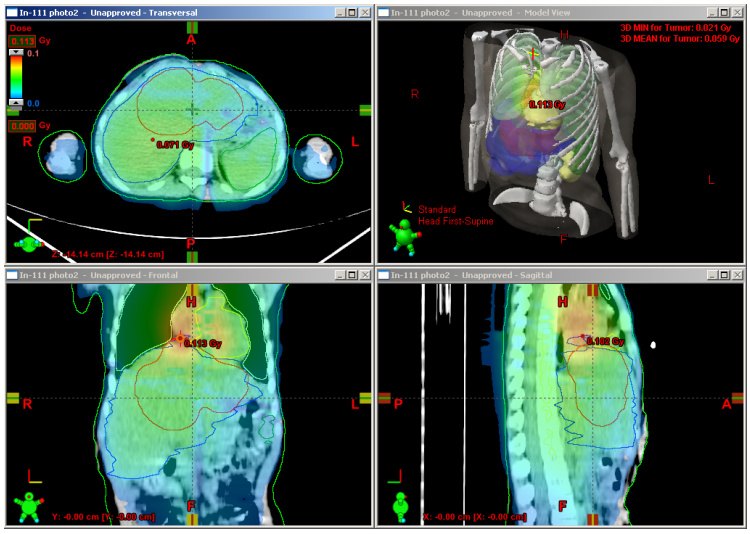

Figure 4.1. A dose distribution for Y-90 radionuclide therapy visualized superimposed with CT image and a 3D rendering of the dose cloud with patient anatomy. Reprinted with permission from IV

.

Further analysis was preformed to compare the patient-specific dose calculation dose kernel method with a widely used MIRD S-factor model method for patients receiving monoclonal antibody therapy in III. The results indicate that on the average the model-based methods agree with the patient-specific method, but looking at an individual patient level there are large variations between the methods.The variation of the macroscopic absorbed dose analysis yielded an average of the minimum doses to be 50% and the average of maximums to be 175% of the average dose in the organ. In some patients, the variation was especially larger in the larger organs such as the liver and spleen. The maximum variation within these organs was found to be 20% – 436%.

The same methods were then applied to a different type of radionuclide therapy of recurrent hepatoblastoma with Y-90 in IV, with results indicating similar patient to patient variations as seen in II and III, pointing to the short-comings of the model-based MIRD S-factor methodology. The calculated MIRD Y-90 doses were for cardiac wall 0.75 Gy, liver 0.62 Gy, spleen 0.51Gy, and bone marrow 0.053 Gy, with the effective whole body dose at 0.18 Gy, i.e. 4.23 mGy/MBq. The patient-specific method demonstrated the mean doses in normal tissues as follows: heart 0.58 Gy, liver 0.48 Gy, spleen 0.37 Gy, and bone marrow 0.34 Gy. Dose volume histograms for the different organs were calculated, for instance the actual

liver tumor dose was in average 0.51 Gy, with a range 0.22-0.96 Gy. A visualization of the calculated doses is shown in Figure 4.1.

4.2 A pencil beam superposition algorithm in external radiotherapy

The development of a PB dose calculation method for external photon therapy was undertaken in V and further refined in VI. The earlier paper outlines the methods and foundations of the density-scaling methodology of the pencil beams and depth-dependent component.

As presented in VI, there is generally a good agreement between the calculations utilizing the presented method and MC simulations in different kind of heterogeneous phantoms. Most of the observed discrepancies were within (2%, 2 mm), where the dose difference is specified with respect to the field Central axis (CAX) $d_{\max}$. Considerably larger deviations were found only in the central axis depth dose of the smallest field size (30×30 mm^2) in the lung slab phantom for the 18 MV beam, where discrepancies in the order of 8% were observed inside the lung insert ($\rho_{\mathrm{w}} = 0.3$). These discrepancies are of comparable magnitude ($\sim5\%$), as observed by Arnfield et al. (2000), for the CCC superposition model in similar situations. The explanation for the discrepancies lies in the fact that in high energy beams of small field size there is a loss of electronic equilibrium on the central axis, which is not modeled with rectilinear kernel scaling approaches. The electronic disequilibrium on the field central axis in the low-density material becomes larger as the field size decreases and the beam energy increases and there are more electrons traveling away from the corresponding volume element on the central axis than towards it.

The re-buildup effect is overestimated in our method on the lung-water interface, as seen in Figure 4.2, which is contrary to other SC models that tend to underestimate the effect. This difference in the algorithm behavior is due to the build-up kernel correction method used in the presented method, which is not used in other SC algorithms. The build-up kernel has been designed such that the build-up between vacuum and water is correctly reproduced, whereas the build-up effect between lung and water is probably smaller, which could explain the observed overestimation in the re-buildup region. Fotina et al. (2009) provided comparisons between AAA and SC methods to MC calculations, that show good agreement for both of the methods with slightly better agreement for the SC method.

In higher density material (bone, $\rho_{\mathrm{w}} = 1.85$) the discrepancies between

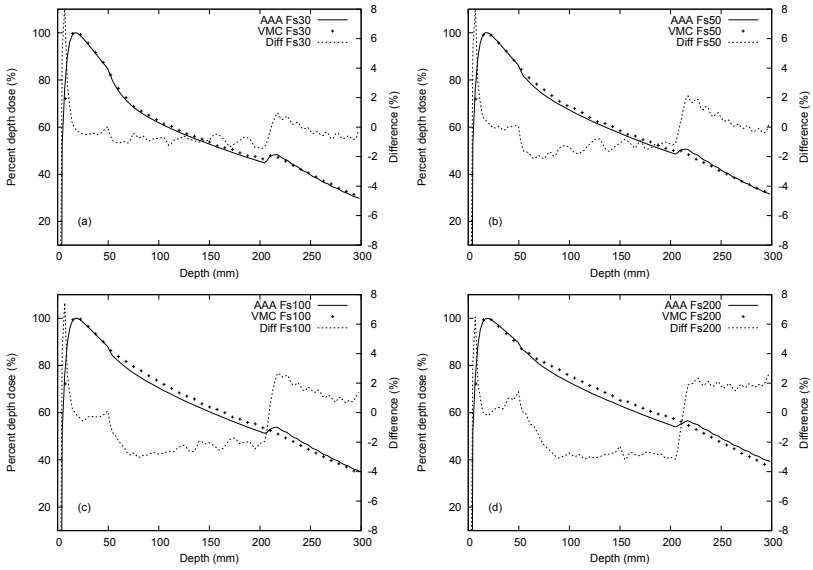

Figure 4.2. Calculated 'AAA' and MC-simulated 'VMC' depth dose curves in the lung slab phantom for the 6 MV beam. (a) Field size $30 \times 30\ \mathrm{mm}^2$, (b) $50 \times 50\ \mathrm{mm}^2$, (c) $100 \times 100\ \mathrm{mm}^2$, and (d) $200 \times 200\ \mathrm{mm}^2$. Reprinted with permission from VI.

our PB algorithm and MC simulations are in the order of (2%, 2 mm). For lower energies (6 MV beam), our method overestimates the dose systematically about 1% inside the high-density material. For higher energy (18 MV), the discrepancies near the heterogeneity border of the bone slab phantom are smaller.

When compared to previously published experimental verification of the presented method, some agreements and some disagreements were found. In the work of Van Esch et al. (2006), the current method was compared to ionization chamber and film measurements in several homogeneous and heterogeneous phantoms. The lateral profile comparisons in the phantom with cork insert are in good agreement with the results in the lung block phantom shown in Figure 4.3. The corresponding depth dose comparisons for 6 MV show a significantly better agreement with the MC simulations in the work than the comparisons to ionization chamber measurements presented by Van Esch et al. (2006). This apparent contradiction can be explained by the fact that the ionization chamber itself can cause significant dose perturbations ($6 \ldots 12\%$) at the point of measurement in case of electronic disequilibrium. These kinds of perturbations occur especially for a small field size, in low-density media.

The main results for the methods in V and VI are that excellent agree-

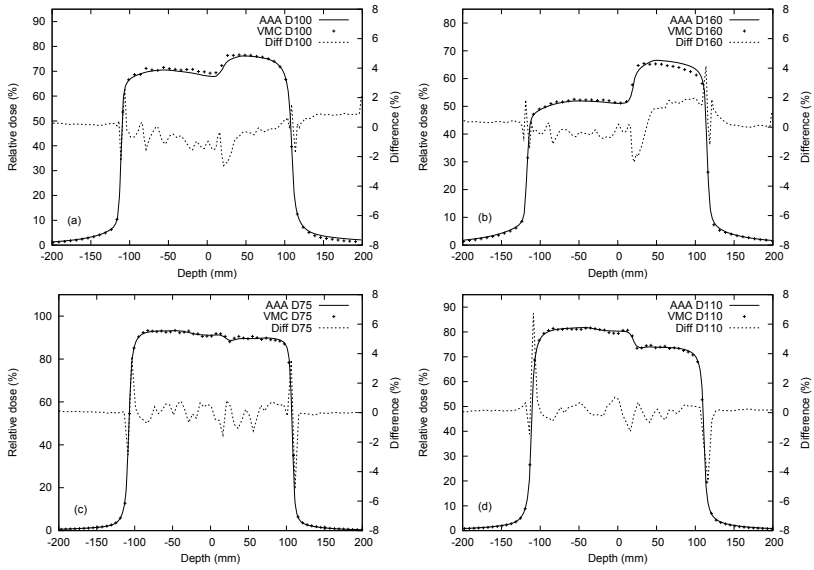

Figure 4.3. Calculated 'AAA' and MC-simulated 'VMC' dose profiles in the lung block phantom for 6 and 18 MV beams. (a) 6 MV, depth 100 mm (b) 6 MV, depth 160 mm, (c) 18 MV, depth 100 mm, and (d) 18 MV, depth 160 mm. Reprinted with permission from VI

ment with MC method and experiments are obtained in homogenous material as well as good results for the lateral heterogeneities (both water-lung and water-bone interfaces) are obtained with lateral scaling of scatter kernels. The method is computationally very efficient for use in a routine clinical setting.

5. Discussion and conclusions

5.1 Overall results

The aims of the Thesis were to develop methods to improve dose calculation in aiding treatment planning of radionuclide and external-beam therapy. The aims of the Thesis were met and a high level summary of results in relation to the aims is presented in Figure 5.1.

The Thesis developed methodology for 3D treatment planning of radionuclide therapy with dose calculation based on quantitative SPECT images and a point dose kernel calculation method. The dose kernel convolution method was applied in several radionuclide therapy cases as a treatment planning and dosimetric verification tool. Comparisons of the developed patient-specific dose calculation method with the widely used MIRD S-factor model was discussed in III and IV. The results show large variations between the methods at individual patient level and within target organs. The results indicate that the spatial dose distribution is needed to further understand therapeutic effect and toxicity of radionuclide treatments, and the developed system is useful in the analysis of radionuclide treatments.

The development of a PB dose kernel based calculation method for external photon therapy that also accounts for local variations in tissue material densities in 3D space was reported in V and further refined in VI. The method performs within clinically acceptable accuracy as compared to experiments and MC calculations with typical agreement within (2%, 2 mm) for various test problems.

Although the aims of the Thesis were met, there is further room for improvement in the source modeling of the radionuclide therapy (i.e. quantitative SPECT and automated processing of time-series activity data).

The recent advances in nuclear medicine imaging with hybrid SPECT/CT devices and PET imaging are enabling this advancement. For instance Willowson et al. (2008) report on an experimental verification of quantitative methodology based on SPECT/CT that achieves accuracy of activity quantification in the range of -7%–%4, compared to known activity concentrations.

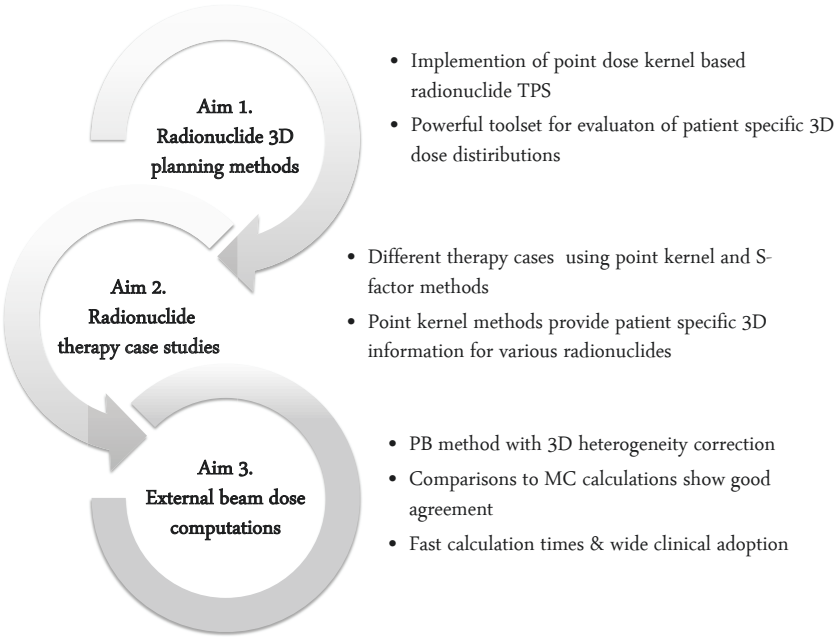

Figure 5.1. Main results grouped by the aims of the Thesis.

5.2 Contribution to the field

This Thesis has developed further computational methods that are relevant in the practical application of radionuclide therapy as well external-beam therapy. Applying the methods in radionuclide therapy has provided new results on the applicability of the methods as well as a comparison to existing practices of the MIRD formalism.

The application of patient-specific dosimetry in radionuclide therapy is still in its infancy in the wider clinical practice of 2016. Although the methods developed as part of this Thesis have been used in clinical practice since 1997, wider adoption will only be possible when these methods are introduced in an easy to use commercial package (by Nuclear Medicine image analysis or general radiotherapy planning software ven-

dors). The work in papers I — IV show that this approach is viable and is well aligned with toolsets available in radiotherapy planning software systems.

In papers V and VI a computationally efficient and accurate PB algorithm was developed with 3D treatment of tissue heterogeneity. It is coupled with an accurate model of the external radiation therapy machine sources including a robust optimization of the model parameters described in Tillikainen et al. (2007). It has been commercialized as the AAA dose calculation algorithm in the widely used Eclipse^{TM} Treatment planning system (Varian Medical Systems, Palo Alto CA). The methods are used in routine clinical practice — with thousands of treatment plans calculated daily using these methods and numerous of studies examining its performance (Ojala et al. 2014; Tsuruta et al. 2014; Liu et al. 2014; Han et al. 2012; Fotina et al. 2009; Breitman et al. 2007; Van Esch et al. 2006, etc.). Its main contribution is the novel treatment of heterogeneity with a good balance between speed and accuracy.

5.3 Future directions

Although more rigorous and complete solutions to the radiation transport exists (see Section 1.6), the model-based superposition and convolution methods continue have an important role in the radiotherapy modeling. In the past two decades, they have been the workhorses for dose calculation as well basis for solutions of the inverse problems. In the future, their computational efficiency will ensure that they have a role in interactive use as well as in radiotherapy plan optimization solutions. The methods also lend themselves for efficient parallel computing implementations, as discussed in Section 3.4.2.

External-beam radiotherapy has transitioned into image guided therapy and the increased information of the daily patient setup will lend itself for adaptation of the treatment plan for the current patient state. This requires advances in rapid and automated dose evaluation, including quick dose calculation and possible treatment plan optimization. These computations need to happen in a few seconds in order not to delay the daily patient treatment. The SC and PB methods are well poised for these scenarios. These needs are also aligned with the adoption of ultra-high dose fractions of the Stereotactic body radiation therapy (SBRT) (Lo et al. 2010).

Further improvements in accuracy could potentially be realized by combining transport equation solvers with extremely fast convolution methods. The approach would perhaps improve the accuracy and modeling of the relevant physics without compromising the speed of the methods to provide fine details of the high resolution shape of the primary photon energy fluence.

Next steps in improving the understanding and radiation dose therapeutic efficacy in radionuclide therapy is to adopt more widely the methods outlined in this Thesis. After that initial step, the next area to improve is the process of acquiring quantitative 3D activity distributions and their use in the patient-specific dose evaluation. Although the accuracy of the dose calculation is currently not the limiting factor, the modeling of the radiation transport could be further enhanced by employing direct solutions to the transport equation by MC methods or deterministic solutions.

5.4 Conclusions

The methods developed in this Thesis have proven to be relevant in the application of radiotherapy. Their relevance for the upcoming improvements in overall radiotherapy applications is also foreseen due to their computational efficiency. Other methods will complement these as the computational power available increases over the upcoming years. Accuracy and efficacy of radiotherapy can be enhanced when physical modeling is further improved and applied in clinical practice.

References

Ahnesjö, A. (1989). "Collapsed cone convolution of radiant energy for photon dose calculation in heterogeneous media." *Med Phys* 16.4, pp. 577–592.

Ahnesjö, A. and M. M. Aspradakis (1999). "Dose calculations for external photon beams in radiotherapy." *Phys Med Biol* 44.11, R99–155.

Ahnesjö, A., P. Andreo, and A. Brahme (1987). "Calculation and application of point spread functions for treatment planning with high energy photon beams." *Acta Oncol* 26.1, pp. 49–56.

Ahnesjö, A., M. Saxner, and A. Trepp (1992). "A pencil beam model for photon dose calculation." *Med Phys* 19.2, pp. 263–273.

Ahnesjö, A., L. Weber, A. Murman, M. Saxner, I. Thorslund, and E. Traneus (2005). "Beam modeling and verification of a photon beam multisource model." *Med Phys* 32.6, pp. 1722–1737.

Andreo, P. (1991). "Monte Carlo techniques in medical radiation physics." *Phys Med Biol* 36.7, pp. 861–920.

Arnfield, M. R., C. H. Siantar, J. Siebers, P. Garmon, L. Cox, and R. Mohan (2000). "The impact of electron transport on the accuracy of computed dose." *Med Phys* 27.6, pp. 1266–1274.

Atun, R., D. A. Jaffray, M. B. Barton, F. Bray, M. Baumann, B. Vikram, T. P. Hanna, F. M. Knaul, Y. Lievens, T. Y. M. Lui, M. Milosevic, B. O'Sullivan, D. L. Rodin, E. Rosenblatt, J. Van Dyk, M. L. Yap, E. Zubizarreta, and M. Gospodarowicz (2015). "Expanding global access to radiotherapy." *Lancet Oncol* 16.10, pp. 1153–1186.

Beekman, F. J., H. W. A. M. de Jong, and S. van Geloven (2002). "Efficient fully 3-D iterative SPECT reconstruction with Monte Carlo-based scatter compensation". *Medical Imaging, IEEE Transactions on* 21.8, pp. 867–877.

Boyer, A. L. (1984). “Shortening the calculation time of photon dose distributions in an inhomogeneous medium.” *Med Phys* 11.4, pp. 552–554.

Boyer, A. L. and E. C. Mok (1985). “A photon dose distribution model employing convolution calculations.” *Med Phys* 12.2, pp. 169–177.

Boyer, A. L. and E. C. Mok (1986a). “Brachytherapy seed dose distribution calculation employing the fast Fourier transform”. *Med Phys* 13, pp. 525–529.

Boyer, A. L. and E. C. Mok (1986b). “Calculation of photon dose distributions in an inhomogeneous medium using convolutions.” *Med Phys* 13.4, pp. 503–509.

Boyer, A. L., Y. P. Zhu, L. Wang, and P. Francois (1989). “Fast Fourier transform convolution calculations of x-ray isodose distributions in homogeneous media.” *Med Phys* 16.2, pp. 248–253.

Breitman, K., S. Rathee, C. Newcomb, B. Murray, D. Robinson, C. Field, H. Warkentin, S. Connors, M. Mackenzie, P. Dunscombe, and G. Fallone (2007). “Experimental validation of the Eclipse AAA algorithm.” *J Appl Clin Med Phys* 8.2, pp. 76–92.

Cade, S. C., S. Arridge, M. J. Evans, and B. F. Hutton (2013). “Use of measured scatter data for the attenuation correction of single photon emission tomography without transmission scanning.” *Med Phys* 40.8, p. 082506.

Carlsson, A. K. and A. Ahnesjö (2000a). “Point kernels and superposition methods for scatter dose calculations in brachytherapy.” *Phys Med Biol* 45.2, pp. 357–382.

Carlsson, A. K. and A. Ahnesjö (2000b). “The collapsed cone superposition algorithm applied to scatter dose calculations in brachytherapy.” *Med Phys* 27.10, pp. 2320–2332.

Chen, Q., M. Chen, and W. Lu (2011). “Ultrafast convolution/ superposition using tabulated and exponential kernels on GPU.” *Med Phys* 38.3, pp. 1150–1161.

Chen, Q., W. Lu, Y. Chen, M. Chen, D. Henderson, and E. Sterpin (2012). “Validation of GPU based TomoTherapy dose calculation engine.” *Med Phys* 39.4, pp. 1877–1886.

Cheng, L., R. F. Hobbs, G. Sgouros, and E. C. Frey (2014). “Development and evaluation of convergent and accelerated penalized SPECT image reconstruction methods for improved dose-volume histogram estimation in radiopharmaceutical therapy.” *Med Phys* 41.11, p. 112507.

Chiavassa, S., M. Bardi, F. Guiraud-Vitaux, D. Bruel, J.-R. Jourdain, D. Franck, and I. Aubineau-Lani (2005). "OEDIPE: a personalized dosimetric tool associating voxel-based models with MCNPX." *Cancer Biother Radiopharm* 20.3, pp. 325–332.

Deng, J., T. Guerrero, C. M. Ma, and R. Nath (2004). "Modelling 6 MV photon beams of a stereotactic radiosurgery system for Monte Carlo treatment planning." *Phys Med Biol* 49.9, pp. 1689–1704.

Dewaraja, Y. K., E. C. Frey, G. Sgouros, A. B. Brill, P. Roberson, P. B. Zanzonico, and M. Ljungberg (2012). "MIRD Pamphlet No. 23: Quantitative SPECT for Patient-Specific 3-Dimensional Dosimetry in Internal Radionuclide Therapy." *J Nucl Med* 53.8, pp. 1310–1325.

Dieudonné, A., R. F. Hobbs, R. Lebtahi, F. Maurel, S. Baechler, R. L. Wahl, A. Boubaker, D. Le Guludec, G. Sgouros, and I. Gardin (2013). "Study of the impact of tissue density heterogeneities on 3-dimensional abdominal dosimetry: comparison between dose kernel convolution and direct Monte Carlo methods." *J Nucl Med* 54.2, pp. 236–243.

Drzymala, R. E., R. Mohan, L. Brewster, J. Chu, M. Goitein, W. Harms, and M. Urie (1991). "Dose-volume histograms." *Int J Radiat Oncol Biol Phys* 21.1, pp. 71–78.

Erdi, A. K., E. D. Yorke, M. H. Loew, Y. E. Erdi, M. Sarfaraz, and B. W. Wessels (1998). "Use of the fast Hartley transform for three-dimensional dose calculation in radionuclide therapy". *Med Phys* 25.11, pp. 2226–2233.

Erdi, E. K., M. Loew, E. Yorke, Y. Erdi, and B. Wessels (1994). "Use of the fast Hartley transform for efficient 3D convolution in calculation of radiation dose". *Proc. 16th Annual IEEE-EMBS Conference*. IEEE. Piscataway, NJ: IEEE, pp. 639–640.

Erlandsson, K., I. Buvat, P. H. Pretorius, B. A. Thomas, and B. F. Hutton (2012). "A review of partial volume correction techniques for emission tomography and their applications in neurology, cardiology and oncology." *Phys Med Biol* 57.21, R119–R159.

Fippel, M., I. Kawrakow, and K. Friedrich (1997). "Electron beam dose calculations with the VMC algorithm and the verification data of the NCI working group." *Phys Med Biol* 42.3, pp. 501–520.

Fippel, M., W. Laub, B. Huber, and F. Nüsslin (1999). "Experimental investigation of a fast Monte Carlo photon beam dose calculation algorithm." *Phys Med Biol* 44.12, pp. 3039–3054.

Fippel, M., F. Haryanto, O. Dohm, F. Nuesslin, and S. Kriesen (2003). “A virtual photon energy fluence model for Monte Carlo dose calculation.” *Med Phys* 30.3, pp. 301–311.

Fix, M. K., M. Stampanoni, P. Manser, E. J. Born, R. Mini, and P. Rüegsegger (2001a). “A multiple source model for 6 MV photon beam dose calculations using Monte Carlo.” *Phys Med Biol* 46.5, pp. 1407–1427.

Fix, M. K., P. Manser, E. J. Born, R. Mini, and P. Rüegsegger (2001b). “Monte Carlo simulation of a dynamic MLC based on a multiple source model.” *Phys Med Biol* 46.12, pp. 3241–3257.

Fix, M. K., P. J. Keall, K. Dawson, and J. V. Siebers (2004). “Monte Carlo source model for photon beam radiotherapy: photon source characteristics.” *Med Phys* 31.11, pp. 3106–3121.

Fix, M. K., D. Frei, W. Volken, H. Neuenschwander, E. Born, and P. Manser (2010). “Monte Carlo dose calculation improvements for low energy electron beams using eMC.” *Phys Med Biol* 55.16, pp. 4577–4588.

Fotina, I., P. Winkler, T. Künzler, J. Reiterer, I. Simmat, and D. Georg (2009). “Advanced kernel methods vs. Monte Carlo-based dose calculation for high energy photon beams.” *Radiother Oncol* 93.3, pp. 645–653.

Furhang, E. E., C. S. Chui, and G. Sgouros (1996a). “A Monte Carlo approach to patient-specific dosimetry”. *Med Phys* 23, pp. 1523–1529.

Furhang, E. E., G. Sgouros, and C. S. Chui (1996b). “Radionuclide photon dose kernels for internal emitter dosimetry”. *Med Phys* 23, pp. 759–764.

Furhang, E. E., C. S. Chui, K. S. Kolbert, S. M. Larson, and G. Sgouros (1997). “Implementation of a Monte Carlo dosimetry method for patient-specific internal emitter therapy”. *Med Phys* 24.7, pp. 1163–1172.

Gardin, I., L. G. Bouchet, K. Assié, J. Caron, A. Lisbona, L. Ferrer, W. E. Bolch, and P. Vera (2003). “Voxeldoes: a computer program for 3-D dose calculation in therapeutic nuclear medicine.” *Cancer Biother Radiopharm* 18.1, pp. 109–115.

Georg, D., T. Nyholm, J. Olofsson, F. Kjaer-Kristoffersen, B. Schnekenburger, P. Winkler, H. Nyström, A. Ahnesjö, and M. Karlsson (2007). “Clinical evaluation of monitor unit software and the application of action levels.” *Radiother Oncol* 85.2, pp. 306–315.

Giap, H. B., D. J. Macey, and D. A. Podoloff (1995a). “Development of a SPECT-based three-dimensional treatment planning system for radioimmunotherapy”. *J Nucl Med* 36, pp. 1885–1894.

Giap, H. B., D. J. Macey, J. E. Bayouth, and A. L. Boyer (1995b). "Validation of a dose-point kernel convolution technique for internal dosimetry". *Phys Med Biol* 40, pp. 365–381.

Grimes, J. and A. Celler (2014). "Comparison of internal dose estimates obtained using organ-level, voxel S value, and Monte Carlo techniques." *Med Phys* 41.9, p. 092501.

Gu, X., D. Choi, C. Men, H. Pan, A. Majumdar, and S. B. Jiang (2009). "GPU-based ultra-fast dose calculation using a finite size pencil beam model." *Phys Med Biol* 54.20, pp. 6287–6297.

Guy, M. J., G. D. Flux, P. Papavasileiou, M. A. Flower, and R. J. Ott (2003). "RMDP: a dedicated package for 131I SPECT quantification, registration and patient-specific dosimetry." *Cancer Biother Radiopharm* 18.1, pp. 61–69.

Halperin, E. C., C. A. Perez, and L. W. Brady (2008). *Perez and Brady's Principles and Practice of Radiation Oncology*. Philadelphia, PA: Lippincott Williams & Wilkins.

Han, T., F. Mourtada, K. Kisling, J. Mikell, D. Followill, and R. Howell (2012). "Experimental validation of deterministic Acuros XB algorithm for IMRT and VMAT dose calculations with the Radiological Physics Center's head and neck phantom." *Med Phys* 39.4, pp. 2193–2202.

Hissoiny, S., B. Ozell, and P. Després (2009). "Fast convolution-superposition dose calculation on graphics hardware." *Med Phys* 36.6, pp. 1998–2005.

Hissoiny, S., B. Ozell, and P. Després (2010). "A convolution-superposition dose calculation engine for GPUs." *Med Phys* 37.3, pp. 1029–1037.

Hubbell, J. H. and S. M. Seltzer (1996). *Tables of X-ray Mass Attenuation Coefficients and Mass Energy-Absorption Coefficients from 1 keV to 20 MeV for Elements Z = 1 to 92 and 48 Additional Substances of Dosimetric Interest*. URL: `http://physics.nist.gov/PhysRefData/XrayMassCoef/cover.html`.

Humm, J. L., J. C. Roeske, D. R. Fisher, and G. T. Chen (1993). "Microdosimetric concepts in radioimmunotherapy". *Med Phys* 20.2 Pt 2, pp. 535–541.

Hutton, B. F., I. Buvat, and F. J. Beekman (2011). "Review and current status of SPECT scatter correction." *Phys Med Biol* 56.14, R85–112.

ICRU (1988). *Fundamental quantities and units for ionizing radiation ICRU Publication 60*. Bethesda, MD: International Commission on Radiation Units and Measurements.

Jackson, P. A., J.-M. Beauregard, M. S. Hofman, T. Kron, A. Hogg, and R. J. Hicks (2013). "An automated voxelized dosimetry tool for radionuclide therapy based on serial quantitative SPECT/CT imaging." *Med Phys* 40.11, p. 112503.

Jacques, R., J. Wong, R. Taylor, and T. McNutt (2011). "Real-time dose computation: GPU-accelerated source modeling and superposition/ convolution." *Med Phys* 38.1, pp. 294–305.

Jia, X., X. Gu, Y. J. Graves, M. Folkerts, and S. B. Jiang (2011). "GPU-based fast Monte Carlo simulation for radiotherapy dose calculation." *Phys Med Biol* 56.22, pp. 7017–7031.

Jia, X., P. Ziegenhein, and S. B. Jiang (2014). "GPU-based high-performance computing for radiation therapy." *Phys Med Biol* 59.4, R151–R182.

Jiang, S. B., A. L. Boyer, and C. M. Ma (2001). "Modeling the extrafocal radiation and monitor chamber backscatter for photon beam dose calculation." *Med Phys* 28.1, pp. 55–66.

Kawrakow, I. and M. Fippel (2000). "VMC++, a fast MC algorithm for Radiation Treatment planning". *The Use of Computers in Radiation Therapy*. Ed. by W. Schlegel and T. Bortfeld. Springer Berlin Heidelberg, pp. 126–128.

Kletting, P., S. Schimmel, H. A. Kestler, H. Hänscheid, M. Luster, M. Fernez, J. H. Bröer, D. Nosske, M. Lassmann, and G. Glatting (2013). "Molecular radiotherapy: the NUKFIT software for calculating the time-integrated activity coefficient." *Med Phys* 40.10, p. 102504.

Kolbert, K. S., G Sgouros, A. M. Scott, J. E. Bronstein, R. A. Malane, J Zhang, H Kalaigian, S McNamara, L Schwartz, and S. M. Larson (1997). "Implementation and evaluation of patient-specific three-dimensional internal dosimetry". *J Nucl Med* 38.2, pp. 301–308.

Kotiluoto, P., J. Pyyry, and H. Helminen (2007). "MultiTrans SP3 code in coupled photon-electron transport problems". *Radiation Physics and Chemistry* 76, pp. 9–14.

Leichner, P. K., K. F. Koral, R. J. Jaszczak, A. J. Green, G. T. Chen, and J. C. Roeske (1993). "An overview of imaging techniques and physical aspects of treatment planning in radioimmunotherapy". *Med Phys* 20.2 Pt 2, pp. 569–577.

Leichner, P. (1994). "A unified approach to photon and beta particle dosimetry". *J Nucl Med* 35, pp. 1721–1729.

Lemaréchal, Y., J. Bert, C. Falconnet, P. Després, A. Valeri, U. Schick, O. Pradier, M.-P. Garcia, N. Boussion, and D. Visvikis (2015). "GGEMS-

Brachy: GPU GEant4-based Monte Carlo simulation for brachytherapy applications." *Phys Med Biol* 60.13, pp. 4987–5006.

Liu, H. H., T. R. Mackie, and E. C. McCullough (1997). "A dual source photon beam model used in convolution/superposition dose calculations for clinical megavoltage x-ray beams." *Med Phys* 24.12, pp. 1960–1974.

Liu, H. H., T. R. Mackie, and E. C. McCullough (2000). "Modeling photon output caused by backscattered radiation into the monitor chamber from collimator jaws using a Monte Carlo technique." *Med Phys* 27.4, pp. 737–744.

Liu, H.-W., Z. Nugent, R. Clayton, P. Dunscombe, H. Lau, and R. Khan (2014). "Clinical impact of using the deterministic patient dose calculation algorithm Acuros XB for lung stereotactic body radiation therapy." *Acta Oncol* 53.3, pp. 324–329.

Ljungberg, M., M. King, G. Hademenos, and S. Strand (1994). "Comparison of four scatter correction methods using monte carlo simulated source distributions". *J Nucl Med* 35, pp. 143–151.

Ljungberg, M., K. Sjögreen, X. Liu, E. Frey, Y. Dewaraja, and S.-E. Strand (2002). "A 3-dimensional absorbed dose calculation method based on quantitative SPECT for radionuclide therapy: evaluation for (131)I using monte carlo simulation." *J Nucl Med* 43.8, pp. 1101–1109.

Lo, S. S., A. J. Fakiris, E. L. Chang, N. A. Mayr, J. Z. Wang, L. Papiez, B. S. Teh, R. C. McGarry, H. R. Cardenes, and R. D. Timmerman (2010). "Stereotactic body radiation therapy: a novel treatment modality." *Nat Rev Clin Oncol* 7.1, pp. 44–54.

Loudos, G., I. Tsougos, S. Boukis, N. Karakatsanis, P. Georgoulias, K. Theodorou, K. Nikita, and C. Kappas (2009). "A radionuclide dosimetry toolkit based on material-specific Monte Carlo dose kernels." *Nucl Med Commun* 30.7, pp. 504–512.

Lubberink, M., H. Lundqvist, J. E. Westlin, V. Tolmachev, H. Schneider, A. Lövqvist, A. Sundin, and J. Carlsson (1999). "Positron emission tomography and radio-immunotargeting – aspects of quantification and dosimetry." *Acta Oncol* 38.3, pp. 343–349.

Lundqvist, H., M. Lubberink, V. Tolmachev, A. Lövqvist, A. Sundin, S. Beshara, A. Bruskin, J. Carlsson, and J. E. Westlin (1999). "Positron emission tomography and radioimmunotargeting–general aspects." *Acta Oncol* 38.3, pp. 335–341.

Ma, C. M., E. Mok, A. Kapur, T. Pawlicki, D. Findley, S. Brain, K. Forster, and A. L. Boyer (1999). "Clinical implementation of a Monte Carlo treatment planning system." *Med Phys* 26.10, pp. 2133–2143.

Macey, D. J., E. J. Grant, J. E. Bayouth, H. B. Giap, S. J. Danna, R. Sirisriro, and D. A. Podoloff (1995). "Improved conjugate view quantitation of I-131 by subtraction of scatter and septal penetration events with a triple energy window method." *Med Phys* 22.10, pp. 1637–1643.

Mackie, T. R., J. W. Scrimger, and J. J. Battista (1985). "A convolution method of calculating dose for 15-MV x rays." *Med Phys* 12.2, pp. 188–196.

Mackie, T. R., A. F. Bielajew, D. W. Rogers, and J. J. Battista (1988). "Generation of photon energy deposition kernels using the EGS Monte Carlo code." *Phys Med Biol* 33.1, pp. 1–20.

Marcatili, S., C. Pettinato, S. Daniels, G. Lewis, P. Edwards, S. Fanti, and E. Spezi (2013). "Development and validation of RAYDOSE: a Geant4-based application for molecular radiotherapy." *Phys Med Biol* 58.8, pp. 2491–2508.

Mohan, R. and C. S. Chui (1987). "Use of fast Fourier transforms in calculating dose distributions for irregularly shaped fields for three-dimensional treatment planning." *Med Phys* 14.1, pp. 70–77.

Mohan, R., C. Chui, and L. Lidofsky (1985). "Energy and angular distributions of photons from medical linear accelerators." *Med Phys* 12.5, pp. 592–597.

Nath, R., L. L. Anderson, G. Luxton, K. A. Weaver, J. F. Williamson, and A. S. Meigooni (1995). "Dosimetry of interstitial brachytherapy sources: recommendations of the AAPM Radiation Therapy Committee Task Group No. 43. American Association of Physicists in Medicine." *Med Phys* 22.2, pp. 209–234.

Neuenschwander, H., T. R. Mackie, and P. J. Reckwerdt (1995). "MMC–a high-performance Monte Carlo code for electron beam treatment planning." *Phys Med Biol* 40.4, pp. 543–574.

Ojala, J. (2014). "Monte Carlo Simulations in Quality Assurance of Dosimetry and Clinical Dose Calculations in Radiotherapy". PhD thesis. Tampere University of Technology.

Ojala, J. J., M. K. Kapanen, S. J. Hyödynmaa, T. K. Wigren, and M. A. Pitkänen (2014). "Performance of dose calculation algorithms from three generations in lung SBRT: comparison with full Monte Carlo-based dose distributions." *J Appl Clin Med Phys* 15.2, p. 4662.

Ott, R. J. (1996). “Imaging technologies for radionuclide dosimetry”. *Phys Med Biol* 41.10, pp. 1885–1894.

Ouyang, J., G. El Fakhri, and S. C. Moore (2007). “Fast Monte Carlo based joint iterative reconstruction for simultaneous 99mTc/ 123I SPECT imaging.” *Med Phys* 34.8, pp. 3263–3272.

Petrokokkinos, L., K. Zourari, E. Pantelis, A. Moutsatsos, P. Karaiskos, L. Sakelliou, I. Seimenis, E. Georgiou, and P. Papagiannis (2011). “Dosimetric accuracy of a deterministic radiation transport based 192Ir brachytherapy treatment planning system. Part II: Monte Carlo and experimental verification of a multiple source dwell position plan employing a shielded applicator.” *Med Phys* 38.4, pp. 1981–1992.

Poon, E., J. F. Williamson, T. Vuong, and F. Verhaegen (2008). “Patient-specific Monte Carlo dose calculations for high-dose-rate endorectal brachytherapy with shielded intracavitary applicator.” *Int J Radiat Oncol Biol Phys* 72.4, pp. 1259–1266.

Pouget, J.-P., C. Lozza, E. Deshayes, V. Boudousq, and I. Navarro-Teulon (2015). “Introduction to radiobiology of targeted radionuclide therapy.” *Front Med (Lausanne)* 2, p. 12.

Pratx, G. and L. Xing (2011). “GPU computing in medical physics: a review.” *Med Phys* 38.5, pp. 2685–2697.

Prideaux, A. R., H. Song, R. F. Hobbs, B. He, E. C. Frey, P. W. Ladenson, R. L. Wahl, and G. Sgouros (2007). “Three-dimensional radiobiologic dosimetry: application of radiobiologic modeling to patient-specific 3-dimensional imaging-based internal dosimetry.” *J Nucl Med* 48.6, pp. 1008–1016.

Reiner, D., M. Blaickner, and F. Rattay (2009). “Discrete beta dose kernel matrices for nuclides applied in targeted radionuclide therapy (TRT) calculated with MCNP5”. *Med Phys* 36.11, pp. 4890–4896.

Rivard, M. J., B. M. Coursey, L. A. DeWerd, W. F. Hanson, M. S. Huq, G. S. Ibbott, M. G. Mitch, R. Nath, and J. F. Williamson (2004). “Update of AAPM Task Group No. 43 Report: A revised AAPM protocol for brachytherapy dose calculations.” *Med Phys* 31.3, pp. 633–674.

Rogers, D. W., B. A. Faddegon, G. X. Ding, C. M. Ma, J. We, and T. R. Mackie (1995). “BEAM: a Monte Carlo code to simulate radiotherapy treatment units.” *Med Phys* 22.5, pp. 503–524.

Rogers, D. W. O. (2006). “Fifty years of Monte Carlo simulations for medical physics.” *Phys Med Biol* 51.13, R287–R301.

Seco, J. and P. M. Evans (2006). “Assessing the effect of electron density in photon dose calculations.” *Med Phys* 33.2, pp. 540–552.

Sgouros, G., G. Barest, J. Thekkumthala, C. Chui, R. Mohan, R. E. Bigler, and P. B. Zanzonico (1990). “Treatment planning for internal radionuclide therapy: three-dimensional dosimetry for nonuniformly distributed radionuclides.” *J Nucl Med* 31.11, pp. 1884–1891.

Sgouros, G., S. Chiu, K. S. Pentlow, L. J. Brewster, H. Kalaigian, B. Baldwin, F. Daghighian, M. C. Graham, S. M. Larson, and R. Mohan (1993). “Three-dimensional dosimetry for radioimmunotherapy treatment planning”. *J Nucl Med* 34.9, pp. 1595–1601.

Sheikh-Bagheri, D. and D. W. O. Rogers (2002a). “Monte Carlo calculation of nine megavoltage photon beam spectra using the BEAM code.” *Med Phys* 29.3, pp. 391–402.

Sheikh-Bagheri, D. and D. W. O. Rogers (2002b). “Sensitivity of megavoltage photon beam Monte Carlo simulations to electron beam and other parameters.” *Med Phys* 29.3, pp. 379–390.

Stabin, M. G., R. B. Sparks, and E. Crowe (2005). “OLINDA/EXM: the second-generation personal computer software for internal dose assessment in nuclear medicine.” *J Nucl Med* 46.6, pp. 1023–1027.

Storchi, P. and E. Woudstra (1996). “Calculation of the absorbed dose distribution due to irregularly shaped photon beams using pencil beam kernels derived form basic beam data.” *Phys Med Biol* 41.4, pp. 637–656.

Storchi, P. R., L. J. van Battum, and E. Woudstra (1999). “Calculation of a pencil beam kernel from measured photon beam data.” *Phys Med Biol* 44.12, pp. 2917–2928.

Strand, S. E., P. Zanzonico, and T. K. Johnson (1993a). “Pharmacokinetic modeling”. *Med Phys* 20.2 Pt 2, pp. 515–527.

Strand, S. E., B. A. Jönsson, M. Ljungberg, and J. Tennvall (1993b). “Radioimmunotherapy dosimetry–a review.” *Acta Oncol* 32.7-8, pp. 807–817.

Tagesson, M., M. Ljungberg, and S. E. Strand (1996). “A Monte-Carlo program converting activity distributions to absorbed dose distributions in a radionuclide treatment planning system.” *Acta Oncol* 35.3, pp. 367–372.

Tedgren, A. K. C. and A. Ahnesjö (2003). “Accounting for high Z shields in brachytherapy using collapsed cone superposition for scatter dose calculation.” *Med Phys* 30.8, pp. 2206–2217.

Tillikainen, L., S. Siljamäki, H. Helminen, J. Alakuijala, and J. Pyyry (2007). "Determination of parameters for a multiple-source model of megavoltage photon beams using optimization methods." *Phys Med Biol* 52.5, pp. 1441–1467.

Tillikainen, L. (2009). "Methods for Dose Calculation and Beam Characterization in External Photon Beam Radiotherapy". PhD thesis. Aalto University.

Traino, A. C., S. Marcatili, C. Avigo, M. Sollini, P. A. Erba, and G. Mariani (2013). "Dosimetry for nonuniform activity distributions: a method for the calculation of 3D absorbed-dose distribution without the use of voxel S-values, point kernels, or Monte Carlo simulations." *Med Phys* 40.4, p. 042505.

Tsuruta, Y., M. Nakata, M. Nakamura, Y. Matsuo, K. Higashimura, H. Monzen, T. Mizowaki, and M. Hiraoka (2014). "Dosimetric comparison of Acuros XB, AAA, and XVMC in stereotactic body radiotherapy for lung cancer." *Med Phys* 41.8, p. 081715.

Tuszynski, J. (2010). *Mass Attenuation Coefficient of Iron with contributions sources of attenuation. Data from XCOM database.* URL: `http://commons.wikimedia.org/wiki/File:Ironattenuation.PNG`..

Van Esch, A., L. Tillikainen, J. Pyykkonen, M. Tenhunen, H. Helminen, S. Siljamäki, J. Alakuijala, M. Paiusco, M. Lori, and D. P. Huyskens (2006). "Testing of the analytical anisotropic algorithm for photon dose calculation." *Med Phys* 33.11, pp. 4130–4148.

Vassiliev, O. N., T. A. Wareing, J. McGhee, G. Failla, M. R. Salehpour, and F. Mourtada (2010). "Validation of a new grid-based Boltzmann equation solver for dose calculation in radiotherapy with photon beams." *Phys Med Biol* 55.3, pp. 581–598.

Verhaegen, F., R. Symonds-Tayler, H. H. Liu, and A. E. Nahum (2000). "Backscatter towards the monitor ion chamber in high-energy photon and electron beams: charge integration versus Monte Carlo simulation." *Phys Med Biol* 45.11, pp. 3159–3170.

Watson, E. E., M. G. Stabin, and J. A. Siegel (1993). "MIRD formulation". *Med Phys* 20.2 Pt 2, pp. 511–514.

WHO (2015). *Cancer, Fact sheet No. 297*. World Health Organization. URL: `http://www.who.int/mediacentre/factsheets/fs297/en/`.

Williams, L. E., G. L. DeNardo, and R. F. Meredith (2008). "Targeted radionuclide therapy." *Med Phys* 35.7, pp. 3062–3068.

Willowson, K., D. L. Bailey, and C. Baldock (2008). “Quantitative SPECT reconstruction using CT-derived corrections.” *Phys Med Biol* 53.12, pp. 3099–3112.

Wong, E., Y. Zhu, and J. Van Dyk (1996). “Theoretical developments on fast Fourier transform convolution dose calculations in inhomogeneous media.” *Med Phys* 23.9, pp. 1511–1521.

Zourari, K., E. Pantelis, A. Moutsatsos, L. Petrokokkinos, P. Karaiskos, L. Sakelliou, E. Georgiou, and P. Papagiannis (2010). “Dosimetric accuracy of a deterministic radiation transport based 192Ir brachytherapy treatment planning system. Part I: single sources and bounded homogeneous geometries.” *Med Phys* 37.2, pp. 649–661.

Zweit, J. (1996). “Radionuclides and carrier molecules for therapy”. *Phys Med Biol* 41.10, pp. 1905–1914.

Errata

Publication IV

The caption in Figure 2. is truncated and the full caption should read as: Regions of interest used to determine the biological clearance of the In-111-labelled MoAb are shown. The body contours are taken on purpose from another imaging to demonstrate that each imaging session may be individual for body contour drawing.

Radiotherapy is an established treatment modality of cancer where radiation is delivered to the patients from internal or external sources. This thesis explores and introduces improvements to computational methods that are used in the application of internal and external radiotherapy. The summary discusses radiotherapy planning and reviews model-based dose calculation methods in internal and external radiotherapy. Treatment planning methods of internal radionuclide therapy are devloped and applied to analyze radionuclide therapy cases. The thesis also reports on the development of a pencil-beam dose kernel -based calculation method for external photon therapy that also accounts for local variations in tissue material densities in 3D space.

Aalto-DD 57/2016

ISBN 978-952-60-6727-8 (printed)
ISBN 978-952-60-6728-5 (pdf)
ISSN-L 1799-4934
ISSN 1799-4934 (printed)
ISSN 1799-4942 (pdf)

Aalto University
School of Science
Department of Neuroscience and Biomedical Engineering
www.aalto.fi